Eco-friendly and cost-effective recycling of batteries for utilizing transition metals as catalytic materials for purifying tannery wastewater through advanced oxidation techniques: A critical review

Abdelrahman M. Ishmael[1], Mohamed A. Nasser[1], Mohamed Abdel-Nasser[1], Habiba A. Hossni[1], Youssef S. Abdel-Hamed[2], M.O. Abdel-Salam[3,4], Soha A. Abdel-Gawad[5] and Rabab M. El-Sherif[5]

[1]Nanomaterials Science and its Applications Program, Faculty of Science, Benha University-Obour Campus, 13518, Benha, Egypt
[2]Mining and Metallurgical Engineering, Faculty of Engineering, Al-Azhar University, Nasr City, 11884, Cairo, Egypt
[3]Analysis and Evaluation Department, Egyptian Petroleum Research Institute (EPRI), Nasr City, Cairo, 11727, Egypt
[4]Central Analytical Laboratories, Nanotechnology Research, Egyptian Petroleum Research Institute 11(EPRI), Nasr City, Cairo, 11727, Egypt
[5]Faculty of Postgraduate Studies for Nanotechnology, Cairo University, Giza, Egypt

REVIEW ARTICLE

Water pollution presents ongoing challenges, prompting an investigation into unconventional methods for the effective removal of persistent pollutants. Transition metal (TM) and their derivatives are commonly used as catalysts in advanced oxidation processes (AOPs) for wastewater treatment due to their adaptable structure, adjustable optoelectronic properties, and strong catalytic performance. This review provides a detailed inspection of the recent progress in utilizing various recyclable TM-based catalysts recycled from used batteries for water purification through AOPs. Firstly, by categorizing different types of water contaminants and introducing the typical structures and compositions of TM and their composites, including nanoparticulate, encapsulated, nanotubular, and layered forms. The synthesis techniques for controlling the morphology, shape, and doping of these structures have also been thoroughly discussed. The latest developments in incorporating TM compounds into AOPs, such as photocatalysis, Fenton-like oxidation reactions, and Persulfate/Oxone activation, have been extensively reviewed. Furthermore, the advantages, limitations, and cost comparisons of various AOPs have been analyzed to support the efficient, environmentally sound, and sustainable removal of organic contaminants from wastewater.

Keywords: Advanced oxidation processes (AOPs); Transition metal (TM); Fenton-oxidation reaction; Photocatalysis

ARTICLE HISTORY
Received: January 07, 2025
Revised: February 12, 2025
Accepted: February 27, 2025

CORRESPONDENCE TO
Soha A. Abdel-Gawad,
Email: soha.gawad@cu.edu.eg
Soha.gawad@yahoo.com
M.O. Abdel-Salam,
Email: m.abdelsalam2008@gmail.com
DOI: 10.21608/nasj.2025.351265.1001

©2025 Cairo University, Faculty of Postgraduate Studies for Nanotechnology

Graphical Abstract

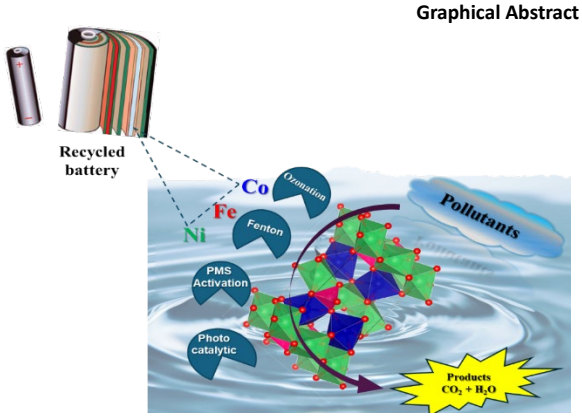

INTRODUCTION

The increasing demand for protecting water ecosystems and reusing treated wastewater has led to extensive research into innovative treatment methods to remove persistent contaminants [1]. While traditional techniques such as adsorption, membrane processes, coagulation, and separation are effective against less persistent pollutants, they are limited by high costs, reduced efficacy against resilient contaminants, and the potential for secondary environmental harm. However, advanced oxidation processes (AOPs) offer a viable solution for efficiently breaking down and detoxifying hazardous persistent pollutants in water systems, making them the most effective and environmentally friendly approach for addressing severe contaminants [2].

The facile formation of various reactive oxygen species (ROSs), like hydroxyl radicals ($OH^{\cdot}$), sulfate radicals ($SO_4^{\cdot-}$), singlet oxygen ($^1O_2$), and superoxide radicals ($O_2^{\cdot-}$) in several AOPs, such as ozonation, UV-based reactions, Fenton-like reactions, electrochemical methods, ultrasound treatment, microwave treatment, and persulfate activation reactions, facilitates the effective breakdown of the organic pollutants originating from diverse industrial sources [3]. Generating these ROSs on catalyst surfaces simplifies operation, reducing costs and enhancing efficiency in eliminating various contaminants compared to alternative methods. Up to now, among various catalyst like quantum dots (QDs), carbon-based materials, polymers, and ceramics, TM compounds such as TM oxides (TMOs), carbides (TMCs), nitrides (TMNs), sulfides(TMSs), dichalcogenides(TMDCs), phosphides (TMPs) , and their combinations have attracted significant attention in this field [4].

TM compounds have been widely utilized due to their abundance in nature, adjustable structures, high electrical conductivity, responsiveness to visible light, impressive thermal and mechanical stability, and effective catalytic properties, particularly in energy conversion and storage sensors , light-emitting diodes (LEDs) , and wastewater treatment applications [5]. AOPs-based TM heterogeneous catalysts have received significant concern, as appears in Figure 1, due to their physicochemical characteristics. Therefore, this review aims to present recent evolutions in novel structures of TM derivatives and their potential for recycling electrodes from used batteries in water purification via photocatalysis, Fenton-like reactions, electrochemical oxidation, and Persulfate/Oxone activation. Additionally, it delves into discussing the key parameters influencing the processes, as well as the advantages, limitations, and cost comparisons of different AOPs in detail.

Classification of dyes and other contaminants

Pollutants, like pharmaceuticals, hormone-disrupting compounds, personal hygiene products, pesticides, and dyes, pose significant challenges to both aquatic and terrestrial environments. The textile industry contributes a diversity of water contaminants, including persistent dyes, emulsifiers, salts, and heavy metals. According to a World Bank report, approximately 17% to 20% of water quality problems are attributed to textile manufacturing processes, particularly during the coloring and finishing stages. Most dyes used in this industry are azo dyes, which form a harmful group due to their persistence and frequent disposal without prior treatment, posing significant risks to human health, aquatic life, and vegetation. These dyes consist of chromophores, responsible for coloring fabrics, and auxochromes, which are used to fix the color on the fibers [6]. As shown in Figure 2, dyes are classified into soluble- and insoluble in water. Soluble dyes may be acidic (anionic), basic (cationic), metalliferous, reactive, and direct dye, whereas insoluble dyes involve sulfur, dispersible pigments, and fixing different dye classes [7].

Structure, Composition, and Synthetic methods for TM catalysts

Structure of TM catalyst

Catalysts composed of TM and their composites exhibit various morphologies to improve the degradation of synthetic organic dyes. The effectiveness of these catalysts is ascribed to their large surface areas and the numerous active sites available on their surfaces. Specifically, encapsulated TM-based catalysts such as core-shell, yolk-shell, mesoporous, nanotubular, and layered structures are particularly noteworthy due to their abundant accessible active sites, which aid in degrading organic pollutants (Figure 3a-e) [8]. For instance, Zhang et al. developed flower-shaped $Li_4Ti_5O_{12}$-TiO_2/C microspheres derived from mulberry leaves, which significantly increased the surface area (Figure 3f, g), while they successfully produced C@TiO_2/3D porous carbon based on porous pollen, providing a broad application prospect (Figure 3h,i) [9]. Other notable architectures include TM oxides and their composites with porous carbons, MXenes, and biological materials, as depicted in Figure 4. Furthermore, Yein et al. described the non-centrosymmetric crystal structure of 2D TM dichalcogenides (TMDCs) piezoelectric materials. These materials have been investigated for wastewater treatment using mono- and persulfate activation techniques as well as Fenton-like reactions [10].

Composition of TM catalyst

Catalysts employed for different AOPs are commonly composed of TM-NPs and encapsulated materials. The versatile combination of various TM-NPs and encapsulated materials substantially promotes the research opportunities of encapsulated TM-based catalysts. Here we will discuss the different composition types for the catalytic performance of wastewater treatment applications.

Composition of TM catalyst with another matrix

The composition of TM and their alloys (binary, ternary, and quaternary alloys) are concisely tuned. Cao *et al.* [11], by synthesizing a TM alloy NP encapsulated in nitrogen-doped carbon (N-C) nanofibers as an effective bifunctional catalyst with altered electronic, catalytic, and chemical characteristics. A series of single atomic TM encapsulated N-C nanotubes (M@N-C, M=Fe, Co, Ni, Cu) were explored for the stable dispersion of metal atoms as promising catalysts. Moreover, the inclusion of heteroatoms can meet the optimum distance between a metal lattice and its atoms, boosting the durability and catalytic efficacy of catalysts. In this regard, numerous studies have recently developed TM-based materials including TMOs. TMOs have been widely proposed in AOPs as low- cost and stable catalysts such as TiO_2, Fe-Mn/ZrO_2, SnO_2, MnO_2, Fe_2O_3, Fe_3O_4, RuO_2, ZnO, and Co_3O_4 [12]. However, TMCs and TMNs demonstrate higher conductivity and better chemical and thermal stability in comparison

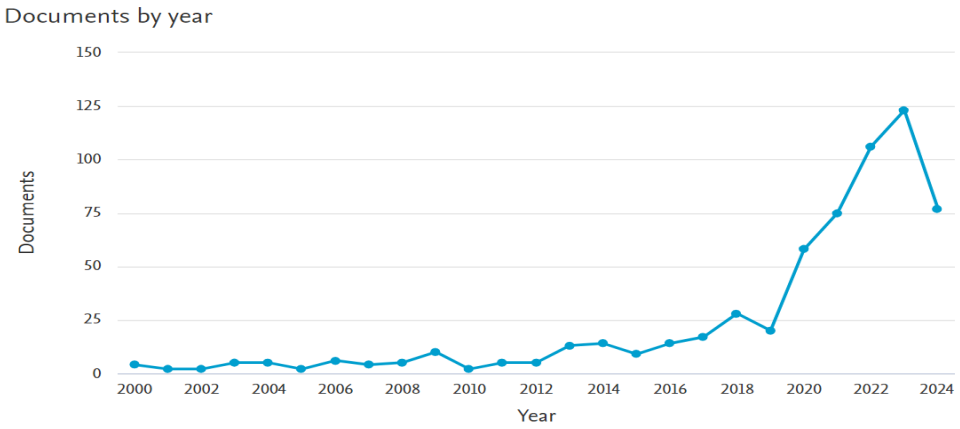

Figure 1. Chart showing the number of publications on AOPs-based TM compounds from 2000 to 2024 based on Scopus database.

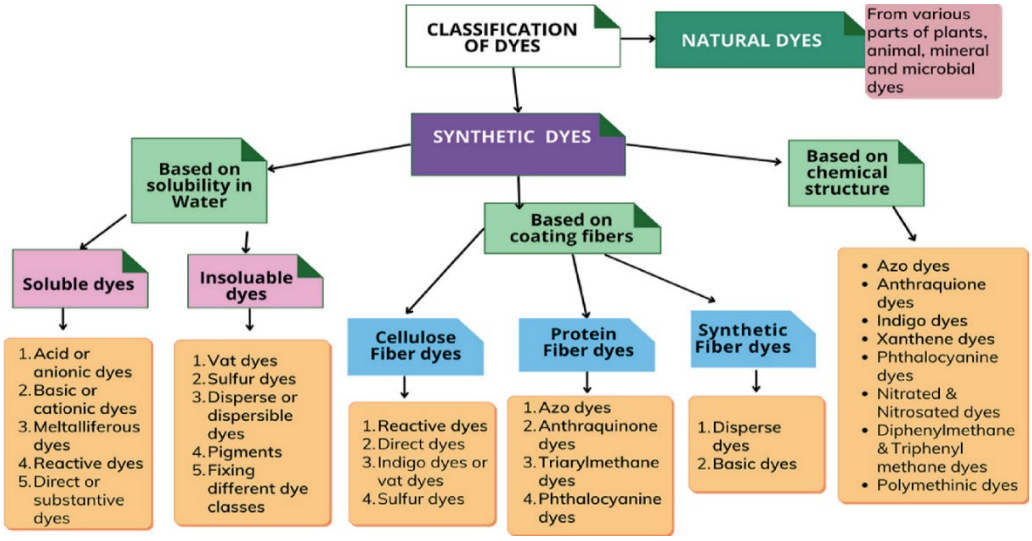

Figure 2. Classification of textile dyes [7].

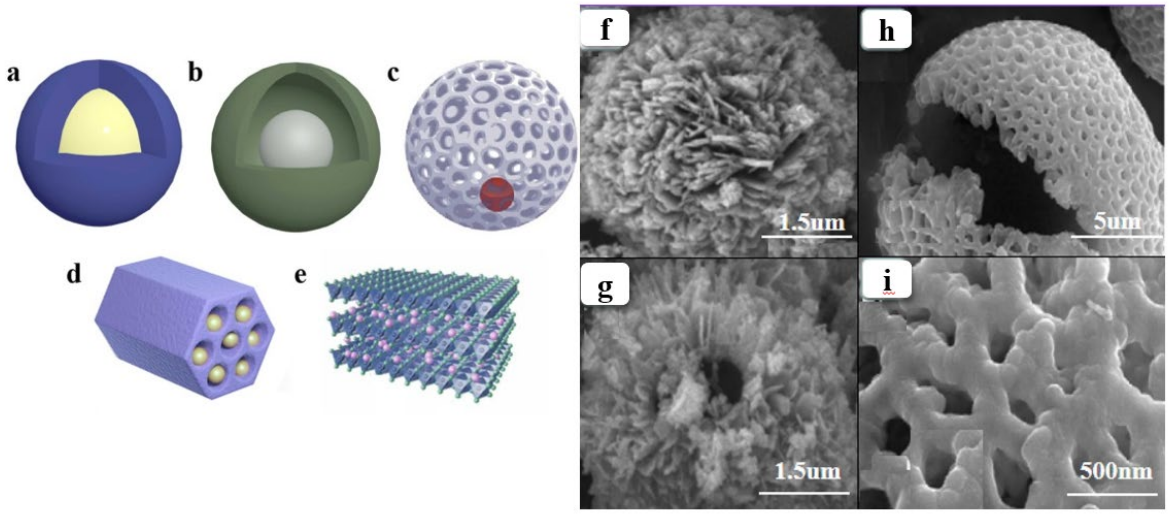

Figure 3. (a) Core-shell structure, (b, c) yolk-shell structure, (d) mesoporous structure, (e) layered structure, (f, g) SEM images of $Li_4Ti_5O_{12}$-TiO_2/C_2. (h,i) SEM images of C@TiO_2/3D pollen carbon (Reproduced with permissions) [*8,9*].

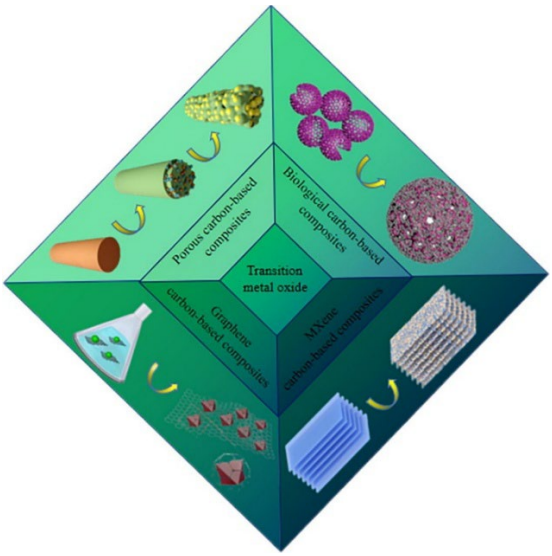

Figure 4. Different morphologies of TMOs-based porous composite materials [10].

to conventional TMOs because of the expansion of their lattices, leading to the contraction of TM d-band, and allowing TMCs to possess Pt-like catalytic behavior [13]. Accordingly, TMPs have better catalytic performance than TM because of their spherical triangular prismatic structure that allows the available exposure of unsaturated surface atoms.

Encapsulated Layer with TM

Because of their distinctive characteristics, carbon-based materials comprising graphene, carbon nanotubes, carbon nanofibers, graphitic carbon nitride (g-C_3N_4), MXenes, metal-organic frameworks (MOFs), and amorphous carbon are the most common forms of embedded layers. Graphene is a 2D layered material of single atomic sheets of carbon atoms connected in the form of sp^2 hybridization comprising a hexagonal ring as the basic unit. When graphene sheets are rolled over each other, 1D carbon nanotubes (CNTs) are formed [14]. G-C_3N_4 resembles graphene in that it possesses a 2D sheet-like structure with a restricted bandgap. Also, due to the sp^2 hybridization, good absorption of solar energy, and the facile diffusion of electrons, g-C_3N_4 is extensively used in photocatalysis for the efficient degradation of organic contaminants. MXenes, a series of 2D TM carbides, nitrides, and carbonitrides with surficial terminated groups such as $^-$OH, $^-$O, and $^-$F that induce hydrophilicity while TM confers the conductivity and the layered structure presents the large surface area, implying them as potential catalysts for wastewater treatment [15].

Synthetic methods for TM-NPs catalysts

Manufacturing TM-NPs catalysts can be done using many synthetic techniques. In general, catalysts of varying structural kinds necessitate distinct synthesis pathways. This section covers various synthetic strategies for TM-NPs catalysts, such as self-assembly, chemical vapor deposition (CVD), thermal, hydrothermal/solvothermal, template-based, and hybrid techniques.

Hydrothermal/solvothermal method

Chemical synthesis in a water or solvent medium at a predetermined temperature and pressure is known as hydrothermal or solvothermal synthesis, and it is frequently employed to create catalysts with a core-shell structure. This process produces a catalyst with a high degree of crystalline, modest strength, and homogeneous dispersion. The catalysts created through hydrothermal/solvothermal synthesis in a confined environment are purer than other synthetic approaches. It also provides a superior environment for crystal development [16].

The reaction temperature, precursor volume, reaction time, and solution pH are the primary control parameters in hydrothermal/solvothermal synthesis. The material's shape and crystallinity are influenced by the temperature and duration of the reaction, which in turn influences the catalyst's activity. For example, when an autoclave's reaction time was reduced from 6 hours to 3 hours while the precursor concentration remained constant, Pd@Fe_3O_4@MOF underwent a morphological transition from yolk-shell structure to core-shell structure [17]. Furthermore, the quantity of precursors has an impact on the activity of reaction nucleation; if the precursor is present in excess, it becomes easier to assemble the active core, which lowers catalytic activity. For instance, dendritic Fe_0@Fe_3O_4 containing polar carbon groups was produced by Xia *et al.* [18]. The volume ratios of ethanol and ultrapure water used had an influence on the catalyst's composition, structure, and catalytic activity. The catalyst changed from Fe_3O_4@Fe_2O_3 to Fe_0@Fe_3O_4 as the ethanol level rose, and the particle-like characteristic formed a dendritic structure with exceptional catalytic capacity towards phenol decomposition.

Anwar *et al.* used a straightforward hydrothermal process to create $Bi_4V_2O_{11}$ and Yb-doped $Bi_4V_2O_{11}$ nanoparticles (Figure 5), which were then characterized and shown to have photocatalytic activity against dye derivatives, methylene blue (MB)

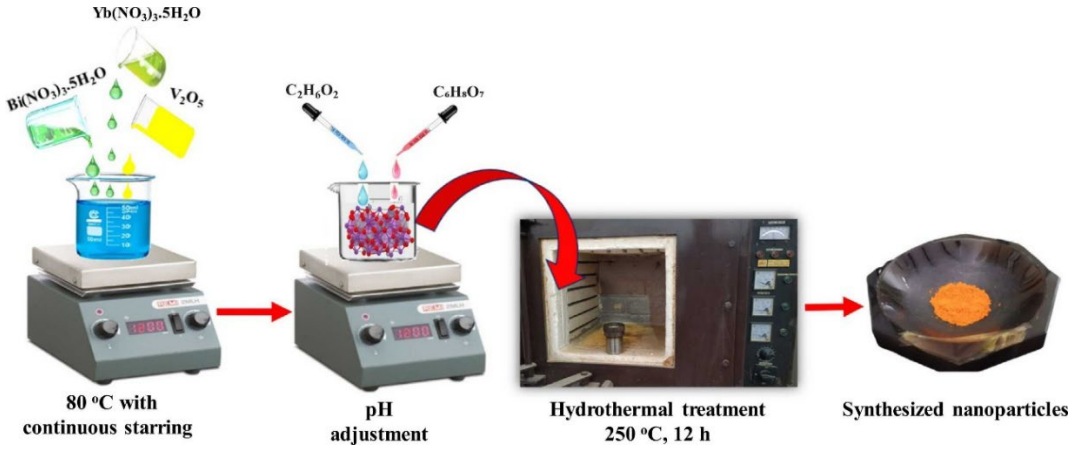

Figure 5. Systematic synthesis routes of $Bi_4V_2O_{11}$ and $Yb/Bi_4V_2O_{11}$ nanoparticles [19].

and Rhodamine B (RhB), under visible light. To increase the $Bi_4V_2O_{11}$ lattice's photocatalytic activity, different amounts of Yb^{3+} ions are doped into it. The phase transition, shape, optical characteristics, photocatalytic activities, and photoluminescence properties were all examined in the produced nanoparticles [19].

Using a solvothermal technique, Naik *et al.* [20]created a CdS/Bi_2S_3 nanocomposite that was coated in Fe_3O_4 nanoparticles and adhered to the surface of reduced graphene oxide (Fe_3O_4@rGO@CdS/Bi_2S_3). To boost catalytic activity, Fe_3O_4 is utilized in this nanocomposite as a magnetic candidate and to produce hydroxy and active oxygen radicals. In addition, under continuous solar radiation, reduced graphene oxide was examined for its ability to function as a shield for metal sulfides and Fe_3O_4 to speed up electron transport in an aqueous solution and cause quick methylene blue dye degradation and hexavalent chromium (Cr (VI)) reduction (Figure 6).

Thermal synthesis

To design TM catalysts with specific characteristics, thermal synthesis techniques provide an efficient path, targeted chemical transformations and phase transitions are created by carefully heating precursors during thermal synthesis, which yields the desired products. Thermal synthesis is a useful technique for producing complex structures, assisted catalysts, and nanoparticles with specific surface characteristics, structures, and shapes in the context of TM catalysts. The primary influencing parameters of thermal synthesis are the temperature of the reaction and precursor nature and proportions, which are very straightforward when contrasted with other synthesizing processes [21].

For example, the catalytic action on biomass, Shen *et al.* [22] employed spent lithium-ion batteries to make char via combustion. Firstly, the spent ternary LIBs (LiNi1/3Co1/3Mn1/3O2, Samsung-CS0400R0003E) were separated discharged, calcined (350 ◦C at a rate of 5 ◦C/min for 30 min in the air), milled, and screened (effectively removing aluminum) to prepare the cathode component (black small powders with particle sizes less than 150 nm). Also, Cao *et al.* [23]directly synthesis $CoFe_2O_4$ nanoparticles via a solution combustion process from ferric nitrate, cobalt nitrate, and glycine were the raw ingredients used as shown in Figure 7. A viable substitute reusable photo-Fenton catalyst for eliminating organic dyes improved by $CoFe_2O_4$.

Chemical vapor deposition (CVD)

CVD serves as a generic gas-phase fabrication nano catalyst method. There are three basic steps in the CVD process: 1) The reaction gases diffuse onto the substrate's surface; 2) The reaction gases adsorb onto the substrate's surface; 3) A reaction occurs on the surface of the substrate, producing gaseous byproducts as well as solid deposits. The homogeneity of the TM catalyst may be precisely regulated by varying factors like reaction gas, reaction temperature, and precursor volume. Notwithstanding the intricate chemical system, CVD is able to manufacture high-density and pristine materials while controlling the carbon constituents' crystal structure, surface morphology, and level of graphitization [24]. Using a straightforward, controllable CVD technique, Dia *et al.* [25] were able to effectively produce nickel sulfide nanoplates with different stoichiometric ratios and high catalytic activity.

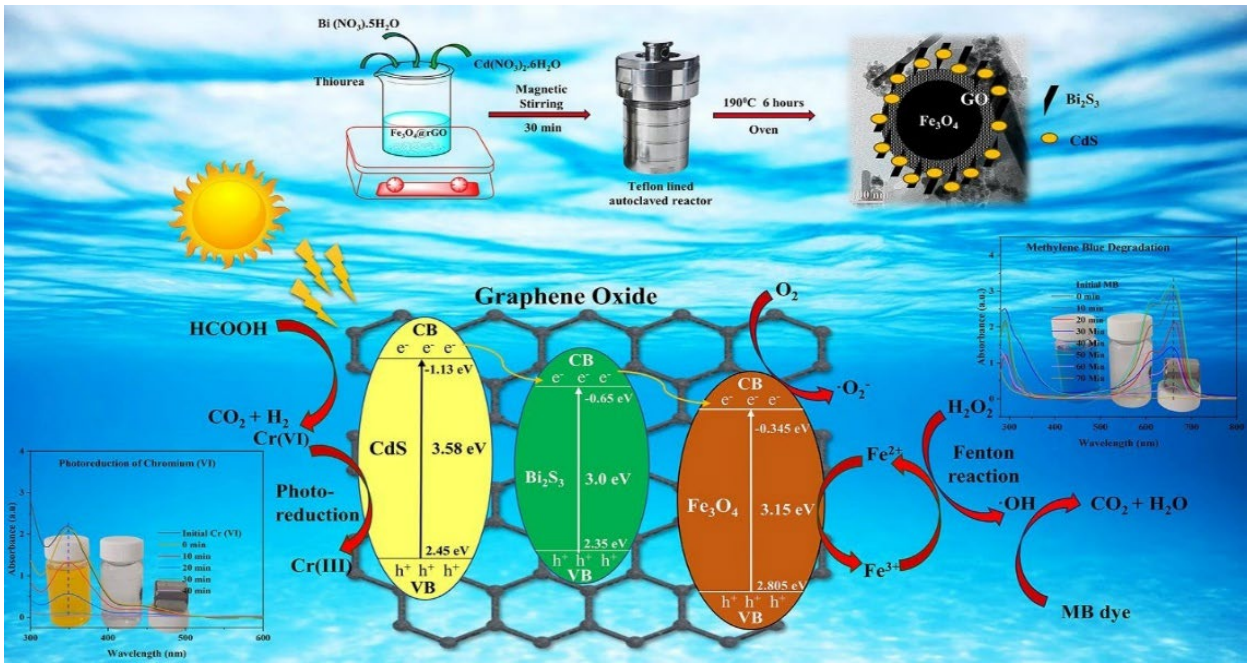

Figure 6. Possible mechanism for photocatalytic Cr (VI) reduction and photo-Fenton MB degradation [20].

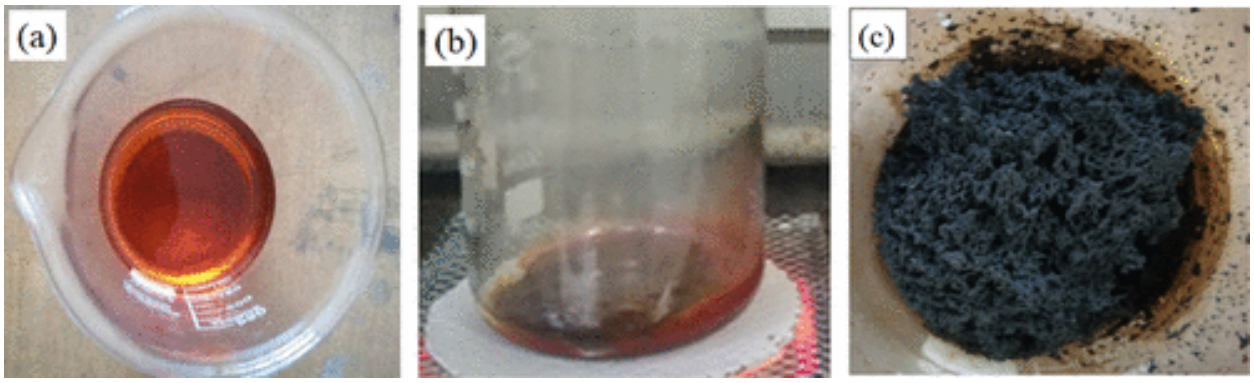

Figure 7. Solution combustion synthesis reaction process of: (a) original solution, (b) formed gel, and (c) final product [23].

The experiment was made of custom-built atmospheric pressure, chemical vapor deposition (APCVD) equipment. Sulfur powder (0.1 g/0.2 g) was placed in the upstream heat zone using a ceramic boat. To promote the growth of nickel sulfide nanoplates, a piece of SiO2/Si substrate was leaned on top of 0.1 g of nickel dichloride powder in an acrylic boat that was placed in the other heat-zone downstream. Ultrahigh-purity argon was purged into a quartz tube for two minutes before heating to eliminate any oxygen and moisture. The two heat zones were then heated to 180–200 °C (upstream) and 520–530 °C (downstream) under a continuous flow of Ar (100 standard cubic centimeters per minute (sccm) and H2 (2 sccm), and it was retained for 10 min for growth.

Template-based method

To create catalysts with a mesoporous structure or yolk shell, template-based methods are frequently employed. The unique distinction between the template-based method and other approaches is the requirement for the introduction of a nanostructured template beforehand, which may effectively regulate the reaction material's size, shape, and composition. The choice of template is crucial in the template-based approach since it dictates how a structure forms and the stability and catalytic activity of the catalyst are frequently determined by its structure. Based on their attributes and distinct confinement effects, templates can be classified as either soft or rigid. Typically, the hard template is the stiff substance held together by the covalent link, while

the soft template is the surfactant aggregates [26]. They are both capable of offering a constrained reaction space. The distinction lies in the fact that a soft template's hollow wall permits materials to permeate both inside and outside, whereas a hard template restricts elements from entering the pore through the template's hole [27]. The hard template technique synthesis process mainly consists of the following steps: 1) Creating a precisely shaped template; SiO_2, carbon, and polymers are examples of common hard templates; 2) functioning of the template surface; The removal of the template can be achieved through heat treatment or selective etching, contingent upon the properties of the substrate [28]. Utilizing silica beads with varying diameters of 20, 500, and 1000 nm as templates, Kim *et al.* [29]produced Fe-doped Co_3O_4 nanostructured anode catalysts for the oxygen evolution reaction (OER). Owing to its poor active area and deteriorating mass transfer, the catalyst made utilizing silica beads with the lowest diameter of 20 nm (FCOT-20) demonstrated low electrocatalytic activity for OER while having a comparatively large specific area (Figure 8). Wu *et al.* [30] described a Fe-Co dual single-atom catalyst (DSAC) synthesis method using soft template-directed interlayer restriction. Two types of amphiphiles, stearic acid (SA) and perfluoro tetra decanoic acid (PFTA), self-assemble into a lamellar micelle to generate a two-dimensional soft template. Between the 2D soft template interlayer and a polypyrrole (Ppy) layer that has been coated afterward, Fe and Co ions are contained. A Fe-Co DSAC known as FeCo-NSC is produced following pyrolysis, in which Fe and Co single atoms are isolated independently on 2D carbon nanosheets through coordination with N and S heteroatoms. The as-prepared FeCo-NSC exhibits more electrocatalytic activity than the monometallic SACs (Fe-NSC and Co-NSC) when used as a cathode for Zn-air batteries (Figure 9).

In conclusion, synthesis techniques for TM catalysts offer a diverse array of approaches, each with its own advantages and applications. Researchers have a wide range of tools at their disposal to tailor the properties of catalyst materials to specific catalytic reactions. These synthesis techniques enable precise control over parameters such as composition, morphology, and surface structure, leading to catalysts with boosted activity, selectivity, and stability. Moreover, the progress of efficient and scalable synthesis methods is crucial for advancing catalysis science and meeting the growing demands of industrial applications. By continually innovating and refining synthesis techniques, they can unlock new possibilities for recycled TM catalysts, driving progress in fields ranging from environmental sustainability to energy production and beyond.

Recycled TM catalysts from used batteries

The demand for TM has extensively risen in the last few decades because of its great performance in diverse applications, especially wastewater treatment. However, the high cost and limited resources restrict their utilization. Thus, the recycling of used batteries is vital for protecting the environment and natural resources. Several studies proposed the separation of lithium and different TMs, including Ni, Co, and Mn, from cathodes of lithium-ion batteries (LIBs). Chen *et al.* [31] followed a hydrometallurgical process for gradient recycling of different metals from $LiNi_{0.3}Co_{0.3}Mn_{0.3}O_2$ (NCM) cathode. Lithium was selectively leached under specific conditions in tartaric acidic media, while TM was dissolved in stoichiometric ratios of diluted sulfuric acid. Similarly, Chang *et al.* [32] stated a novel approach to accomplish high recovery of Ni, Co, and Mn from NCM using deep eutectic solvent (DES) containing choline chloride and oxalic acid (ChCl–OA) at 120 °C for 10 h in the form of NiO, Co_3O_4, and Mn_3O_4 with high recovery yields of 99.1 %, 95.1 %, and 95.3 %, respectively as presented in Figure 10. Wang and coauthors have also used a mechanochemical processing technique for the selective separation of critical metals involved in ($LiFePO_4$:NMC,1:1) using choline chloride–formic acid through the combination of DES and the mechanochemical reaction [33]. In addition, Jin *et al.* [34] have proposed a green process for extracting valuable metals from NCM523 by roasting using waste copperas as reducing and sulfating agent. Moreover, during the roasting process, waste copperas broke down into insoluble Fe_2O_3 that can be easily separated as shown in Figure 11.

Applications of TM-NPs catalysts in advanced oxidation processes (AOPs)

Due to the chemical and energy input demands, the utilization of TM-NPs catalysts possesses remarkable physicochemical characteristics that meet the demand of AOPs despite their ability to produce in situ reactive oxygen species (ROS). In this section, the recent progress of TM-NP catalysts in different chemical and physical AOPs for the degradation of aqueous organic pollutants is presented, as shown in Figure 12.

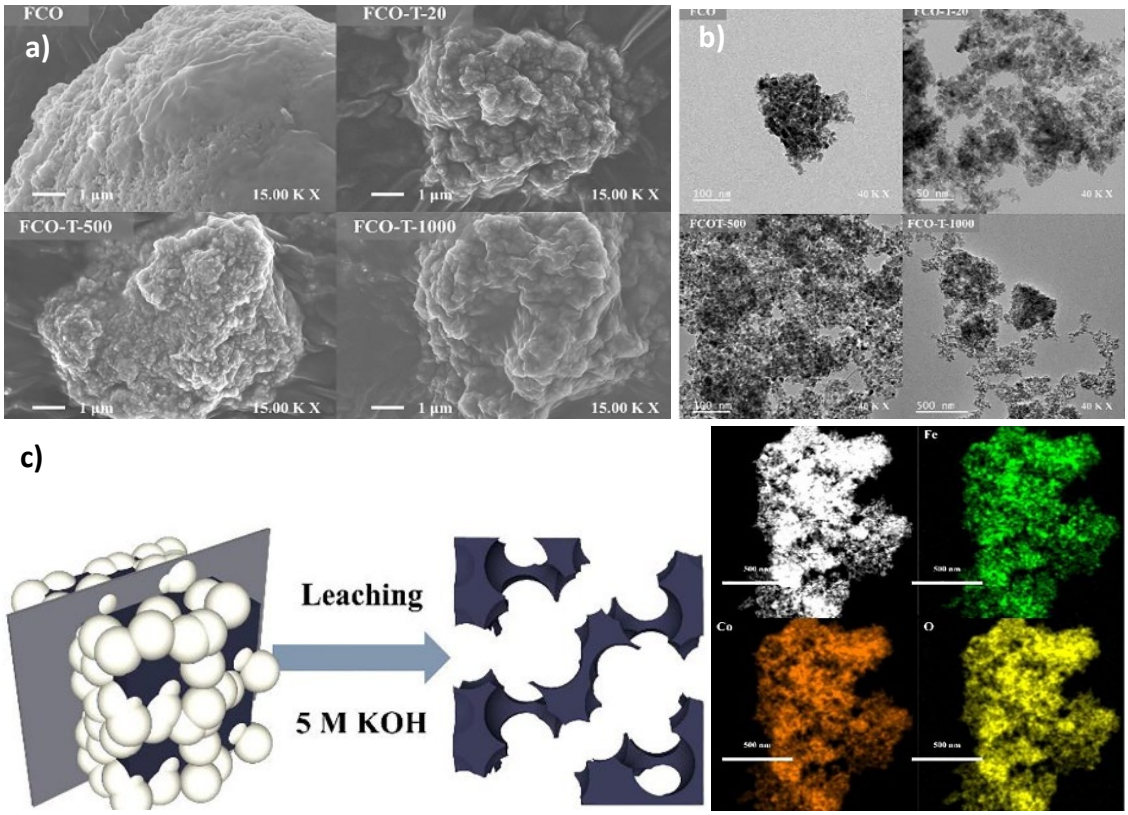

Figure 8. (a), (b) SEM and TEM images of FCO and FCO-T-X. (c) A schematic illustration of pore size-controlled catalysts prepared using a hard-templated method and leaching. (d) EDX images of FCO-T-500 [Fe (green), Co (orange), and O (yellow)] [29].

Chemical AOPs process
Catalytic ozonation

Catalytic ozonation is acquiring interest due to its ability to enhance organic component removal by promoting O_3 breakdown and producing active free radicals through heterogeneous and homogenous catalytic ozonation, which is primarily catalyzed by TM. Furthermore, both heterogeneous and homogeneous catalytic ozonation have shown promise for laboratory-scale removal of dye effluent, with lower ozone demands compared to ozonation alone, which is able to perform much more oxidation than molecular ozone. So, ozone-resistant contaminants may be lessened by O_3 oxidation; therefore, catalysts can increase the conversion of O_3 into reactive oxygen species (ROS), which can help clean water and reduce superoxide radicals [35].

The research studied the catalytic activity of Fe (II) and Co (II) in deionized and dechlorinated natural drinking water from para-chloro benzoic acid (p-CBA) at pH=7.8 at low catalyst concentration as shown in Figure 13 (a, b) specially hydrophobic metals with poor solubility may oxidize and produce nano-scale oxides, by increasing metal concentrations of Co(II) and Fe(II) enhance degrading of p-CBA. Moreover, adding Co (II) to water matrixes containing scavenging chemicals, such as dechlorinated natural potable water, had the opposite effect on the removal of the p-CBA. In comparison to single ozonation, only Fe (II) may be considered a catalyst for the elimination of p-CBA. On the other hand, homogeneous AOPs have a few drawbacks, such as pH dependency, high expense, and difficulty recovering metal ions [36]. Therefore, current research focuses on enhancing the performance of traditional AOPs employing heterogeneous catalysts , with 25% more efficient than ozonation alone using magnetic manganese ferrite particles , nanomaterials , and metal oxides [37].

Recently, the Ag-Ce-O composite metal oxide catalyst was produced by removing reactive black 5 dye (RB5) from textile effluents using the co-precipitation process, in under 80 minutes, the catalyst achieved an 88% chemical oxygen demand removal efficiency Figure 14, eliminating the RB5 dye. Most studies are still ongoing in laboratories, highlighting the need to enhance usage efficiency and address potential ecological concerns such as waste and loss [38].

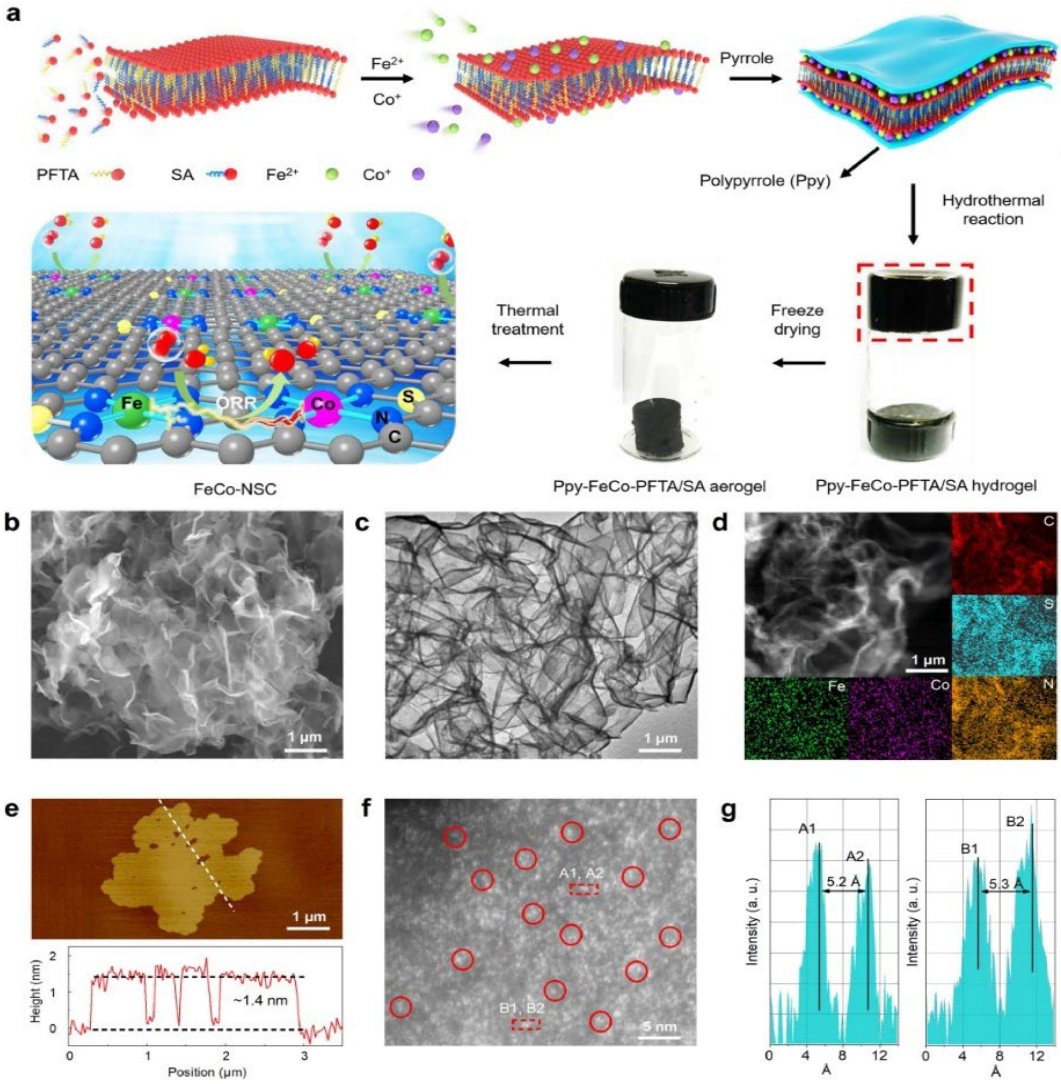

Figure 9. (a) Schematic illustration of synthesis procedure for the FeCo-NSC. (b) SEM and (c) TEM images of FeCo-NSC. (d) HAADF-STEM image and corresponding element mapping of FeCo-NSC. (e) AFM image and corresponding height profile of FeCo-NSC. (f) AC-HAADF-STEM image of FeCo-NSC. Some bimetallic Fe-Co sites are highlighted by red circles. (g) The intensity profiles were obtained on two bimetallic Fe-Co sites [30].

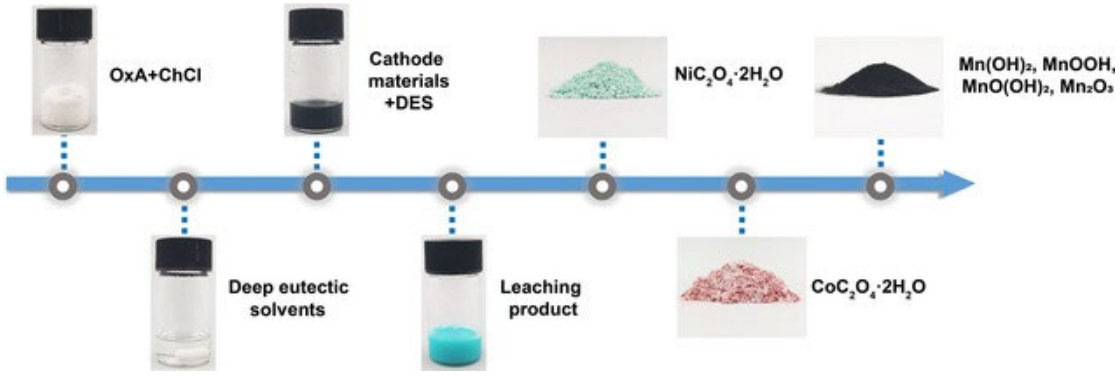

Figure 10. Selective separation of Ni, Co, Mn from spent LIBs [32].

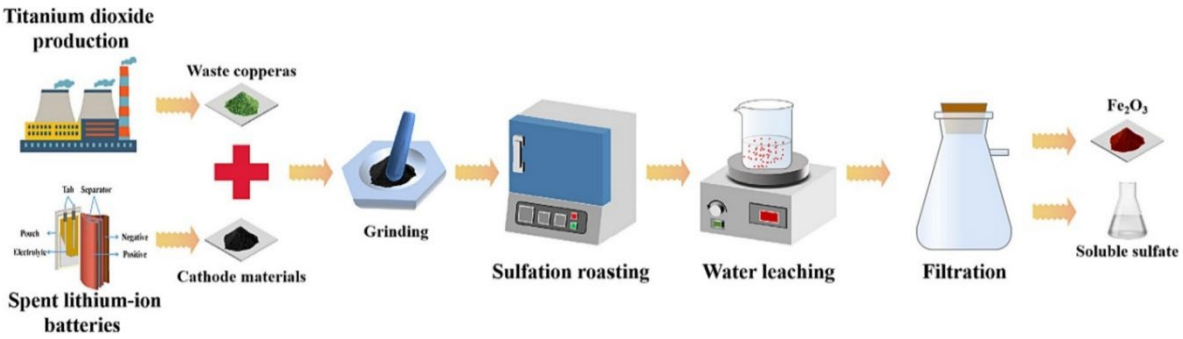

Figure 11. Novel process for extracting valuable metal elements from NCM523 [34].

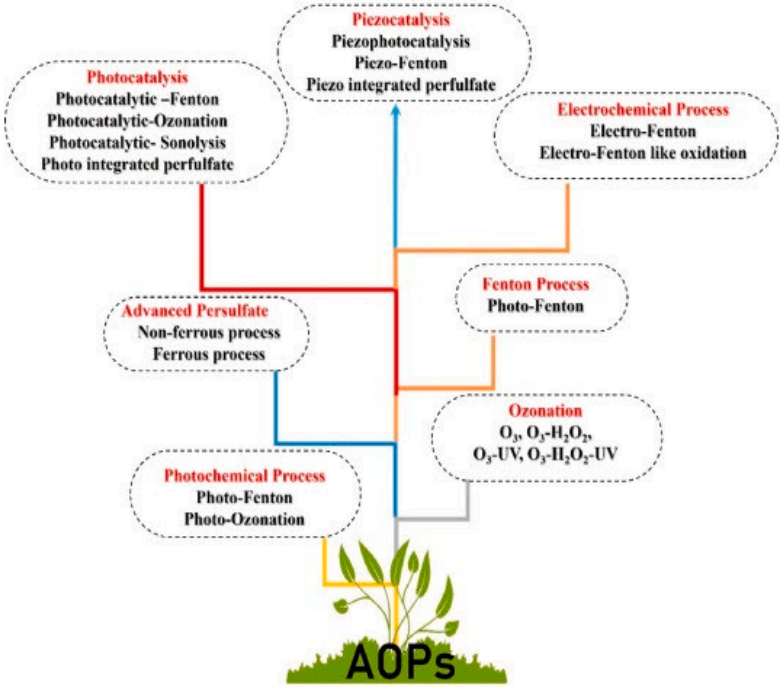

Figure 12. Different AOP processes for generating ROS [10].

Ozonation at elevated pH

PH is an important component of ozonation, it affects ozone breakdown. Ozonation involves two processes: indirect interaction with radical species and direct reaction with ozone. Ozone interacts with certain substances at low pH values, while reactive hydroxyl radicals are the main oxidant at high pH values. Research on its impact on catalytic ozonation is essential for understanding the process [39]. Herein, Mn^{2+} and Co^{2+} at pH 5.5, exhibited a slight rise in efficiency for the breakdown of citric acid by ozone, but Ti^{4+} and Fe^{2+} showed negligible effects with no discernible efficiency at pH. Therefore, the type of catalyst determines the impact on pH. Furthermore, once the pH of the solution was raised from 6 to 7, the percentage of color removal dropped from 93% to 86% and then progressively climbed to 99% at a pH of 10 at concentration of 200 mg/L. Ozone reacts quickly with textile dyes, and pH has a major effect on how quickly dye decolorizes, but the pH's ability to raise the reaction rate while decreasing ozone efficiency [40].

Peroxone-process (O_3/H_2O_2)

The reaction of O_3 with H_2O_2 can produce 50% yield of hydroxyl radicals, accelerating the breakdown of O_3. H_2O_2 is a key initiator in the ozonation process, and HO_2 ions separate from them are more capable of starting and accelerating O_3 breakdown than OH ions. Especially when adding H_2O_2 which increases the rate constant of O_3 consumption by propagation reactions, but its effectiveness hinges on the water matrix and the amount of O_3 supplied. As a result, using TMs (O_3 + H_2O_2 + catalyst system) to assess the

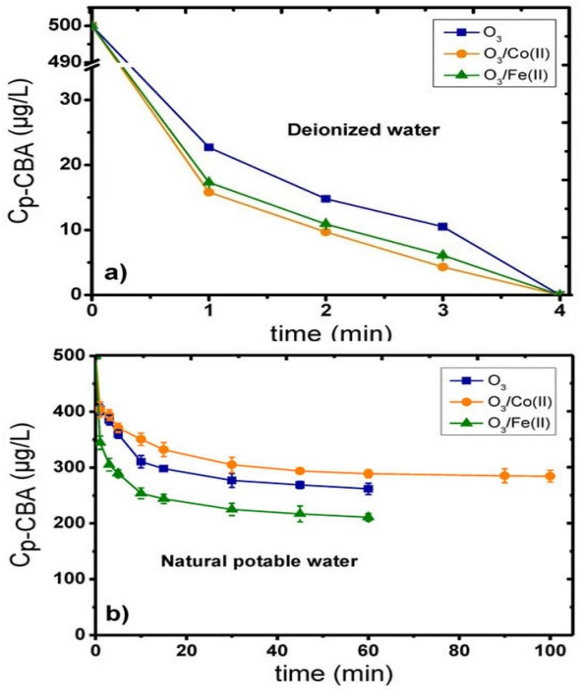

Figure 13. Catalytic ozonation of benzotriazole with the presence of Fe (II) and Co (II) as catalysts, using (a) demonized and (b) dechlorinated natural potable water. Experimental conditions: initial benzotriazole concentration 500 µg/L, ozone concentration 2 mg/L, catalyst concentration 1 mg/L, pH 7.8, temperature 23 ± 2 °C solution comb [*36*].

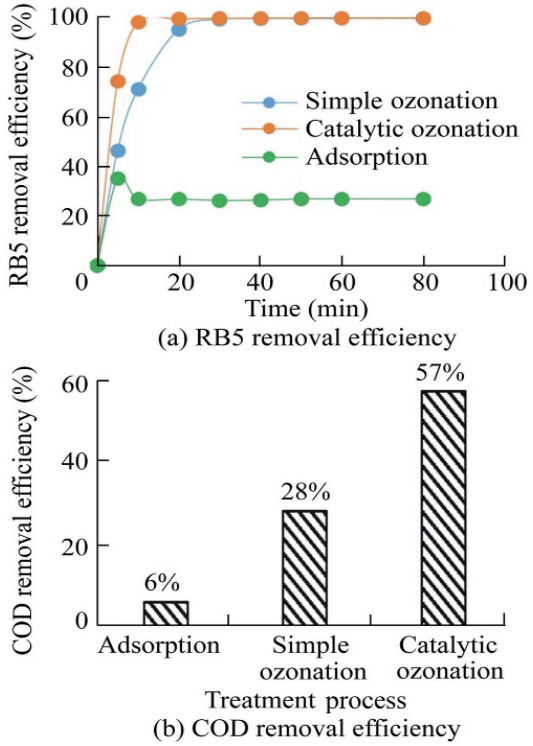

Figure 14. RB5 and COD removal using adsorption, simple ozonation, and catalytic ozonation processes (RB5 concentration of 100 mg/L, pH of 7, catalyst dosage of 0.5 g/L, ozone flow rate of 30 L/h, and reaction time of 80 min) [*38*].

effectiveness of ozone-based advanced oxidation processes by measuring the propagation reaction's promoting impact is found a promising removal, leading to the generation of more hydroxyl radicals than H_2O_2/O_3 as zero valent iron , and titanium [41]. Recently, the Mn-CN catalyst overcomes the limitation of generating OH in acidic solutions by changing the reaction pathway. The catalyst's catalytically active sites are $Mn{-}N_4$, which are formed when a single Mn atom coordinates with four N atoms simultaneously. This site is inactive in O_3 or H_2O_2 activation. Hence, the H_2O_2 adsorbs at this site, creating the $HOO{-}Mn{-}N_4$ species, which combines with the O_3 molecule to generate $HO_2^{\bullet}$ and $O_3^{\bullet-}$, giving $OH^{\bullet}$ as seen in Figure 15, which show significantly greater activity [42]. When Ti(IV) is added to an acetic acid(HAc) solution in an acidic environment, the oxidation efficiency of H_2O_2/O_3 is considerably increased, the removal rate of HAc reaching 62.9% with a typical pesticide degradation yield of 36% in water [43].

UV-based AOPs

Many studies have been investigated on targeting most organic compounds using ultraviolet-based advanced oxidation processes (UV-based AOPs) with rate constants fall between 10^6 and 10^9 $dm^3\ mol^{-1}\ s^{-1}$ respectively, by water photolyzing radical precursor compounds (RPCs) that generate $OH^{\bullet}$ radicals for vacuum UV irradiation, with factors affecting its performance including: 1) the target contaminant's capacity for absorption, 2) the energy needed for photochemical processes, and 3) the indirect or sensitized photolysis of the water quality [44]. However, dissolving carbon dioxide, photo-AOPs are a viable technique for reaching zero-pollution targets. Among these RPCs are UV/persulfate, and UV/H_2O_2, which are most selected for co-effectiveness [45]. For best outcomes, ideal process variables and energy-efficient UV lamps are required. Advancements in material science have generated new potential photo-AOPs which are more effective than traditional AOPs that are covered in this section.

UV/H_2O_2

AOPs using UV/H_2O_2 have shown efficacy for removing the trace of organic pollutants and industrial effluents, which might improve mineralization and aerobic biodegradation by the breakdown of the H_2O_2 bond to generate hydroxyl. A lower starting chemical concentration and a higher H_2O_2 concentration with lower PH were also shown to positively affect the degradation rate constants [46].

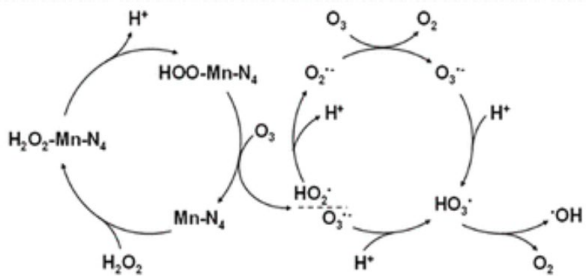

Figure 15. Reaction mechanism in the Mn−CN catalytic peroxone reaction [*42*].

Moreover, it is a useful, environmentally safe method of treating volatile organic compounds and haloacetonitrile (HAN) precursors. The unstable and active hydroxyl radical, high energy consumption, chemical expense, and limited UV transmittance are found tend the researcher to use catalytic activation [47]. As H_2O_2/UV-activated copper oxide nanoparticles, increases the tendency for biodegradation. Additionally, zerovalent iron Fe°/H_2O_2/UV is utilized for color degradation dyes in contaminated water, yielding the greatest mineralization with degrees (70%–80%). About 100% decolorization, the concentration of 0.5 w/w after 8 minutes by adding TiO_2/UV/H_2O_2.The dye's absorption is impacted by the reduction in dye adsorption on TiO_2 that occurs when H_2O_2 concentration rises is achieved. On the contrary, the non-degradable organic compounds reaction of UV-H_2O_2 is faster than using TiO_2/UV/H_2O_2 [48].

UV/SO4$^{\bullet-}$

Persulphate-based oxidation produces sulphate radicals to degrade contaminants with a comparable redox potential to hydroxyl with longer half-life duration (3-4 × 10^{-5} s for $SO_4^{\bullet-}$ vs. 2 × 10^{-8} s for $HO^{\bullet}$), When exposed to UV light (catalyzed part), persulfate functions as an electron acceptor, making it a stable and affordable substitute for eliminating a variety of pollutants, compared to hydrogen peroxide, which works in a variety of pH ranges [49]. The research underlined how crucial the catalyst amount is to the reaction rate to greater pollutant adsorption, more active sites and generate electrons and holes in the oxidative valence band. Within 90 minutes, Dakha et al. [50] reported 98.9% methyl paraben removal ; this process was also shown to be time-efficient, using 54.2 kWhm^3 of energy. Krawczyk et al. [51] reported that in about 60 minutes, treatment with a 2.5 mM solution of the model dye Acid Blue 129. SO4•− effectively decolored 25 mg/L of the dye up to 87%. Recently, UV/Persulfate resulting in almost full destruction of methyl orange (MO) and rhodamine B (RhB) after 5 minutes and total degradation of methylene blue (MB) at 10 µM after 10 minutes in the study of Hoang et al. [52].

Electrochemical AOPs

Electrochemical advanced oxidation processes (EAOPs) are a low-volume, simple method for decontaminating organic contaminants with toxic substances such as herbicides, pesticides, azo dyes, insecticides, and minor acids. Therefore, in EAOPs, the in situ production of a powerful and nonselective radical, $^{\bullet}OH$, for the breakdown of larger molecular weight molecules into lower molecular weight compounds and its mineralization is produced either directly by anodic oxidation (AO) or indirectly through the electrochemical synthesis of Fenton's reagent [53]. Wherein the mechanism discussed in detail here. Nevertheless, depending on the anodic substance, creating stable electrode materials may degrade contaminants. Among the anodes studied so far, boron-doped diamond (BDD) has been shown to be the most effective for its ability to completely degrade organic pollutants due to its minimal adsorption of any molecule. But they have several serious drawbacks, including high power consumption, poor machinability, and high production costs [54].

TMs are found to improve and optimize the electrodes. Herin, the electrochemical active surface area and catalytic oxidation of organic pollutants get improved when Ti/La_2O_3-PbO_2 as an electrode, especially (10:2) %, showed the highest current value and biggest CV curve area (Figure 16a, b) [55]. The $NiCo_2O_4$ nanoarray cathode accelerated the oxidation of peroxymonosulfate (PMS) to break down rhodamine B(RhB), who's the decolorization efficiency increased to 73.3% without the use of electrochemistry (EC). On the other hand, heterogeneous CuO-Co_3O_4 catalysts were assessed for oxidizing ammonia (NH_3) after being created using a co-precipitation technique. affect NH_3 degradation considerably within 65 minutes, with the best Cu/Co ratio increasing the degradation efficiency and a 1:1 Cu/Co ratio obtaining 92% elimination efficiency (Figure 16c) [56].While using a 3D-hexagonal Co_3O_4 anode electrode with 0.5% Co using PMS solution, which reaches a greater removal of 4-nitrophenol(NP),and the formation mechanism were discussed in Figure 16d, the stability of the electrode was stable in the process of coupling the NP with Co_2 [57].

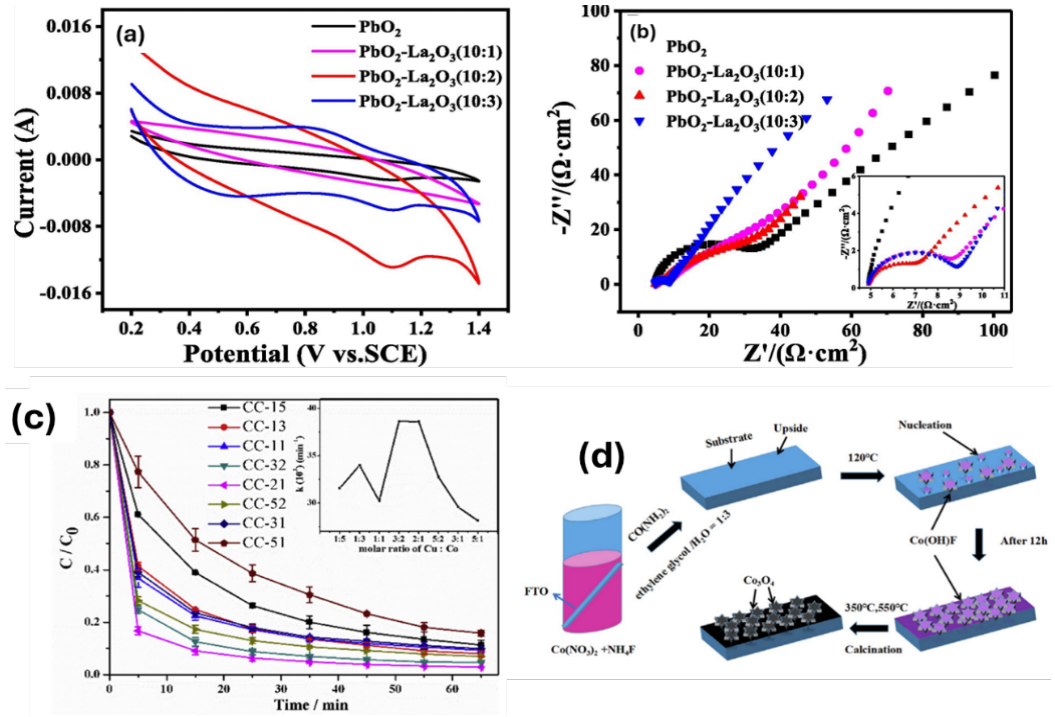

Figure 166. (a) CVs of different anodes obtained in 0.1 M Na_2SO_4 solution, (b) EIS of different anodes obtained in 0.1 M Na_2SO_4 solution, (c) Effect of molar ratio of Cu/Co, and (d) the formation process of 3D-hexagonal Co_3O_4 arrays (Reproduced with permissions) [*55-57*].

Fenton reaction

Fenton-like process

The classical Fenton reaction is a model for heterogeneous Fenton-like reactions. Although the traditional Fenton process is widely used in wastewater treatment plants, it has several inherent drawbacks, including a limited optimum pH range, high operational costs, accumulation of Fe-dense sludge, poor recycling and reusability, and significant iron leaching. As a result, many heterogeneous Fenton-like catalysts have been amplified to replace the traditional Fenton process. Due to their substantial impact on the oxidation capacity of Fenton-like reagents, pH, H_2O_2 dosage, catalyst dosage, and reaction temperature have all been extensively researched. As a result, it is essential to introduce and analyze these factors systematically [58]. According to several studies, a pH of ~3 is still optimal for heterogeneous Fenton-like reactions. For example, the application of Fe-based heterogeneous Fenton-like catalysts for the treatment of wastewater has shown great promise. To learn more about how primary reaction features, such as the starting pH, affect sulfamethoxazole (SMX) degradation as reported in the Fe@MesoC/H_2O_2 system [59]. Experiments were carried out in the pH range of 3.0–5.6 to investigate the impact of the starting pH on SMX degradation. Over the pH range of 3.0 to 4.0, SMX decomposed extremely quickly, with full elimination of the compound occurring in less than 120 minutes of reaction time. The removal efficiency dramatically decreased at pH values of 4.5 and 5.6, and at pH 5.6, 49% of the SMX was eliminated in 120 minutes. The alteration of the H_2O_2 breakdown pathway with increasing pH is one possible cause. Additionally, Fe@MesoC demonstrated strong catalytic activity at a pH of 4.0, suggesting that the catalyst has a wider pH range of operation. Different pH values were employed to assess the validity of methylene blue dye removal by Yolk-shell Fe_3O_4@MOF-5 nanocomposites as a heterogeneous Fenton-like catalyst for methylene blue dye removal. The results demonstrated how the initial pH of the solution affects the effectiveness of methylene blue removal. At an initial pH of 3.0, the removal efficiency of methylene blue reached 100% in just 20 minutes, and at pH 4.0, it reached 100% in 60 minutes. The clearance effectiveness of methylene blue significantly decreased as the pH increased. At pH 7.0, the clearance effectiveness of methylene blue was only 45% after 60 minutes [60].

Other studies have shown that neutral conditions or even alkaline conditions could improve the efficacy of wastewater treatment from several research teams produced disparate research results. It was demonstrated that the application of Fe^0-Fe_2O_3/OMC

and Cu-MP NC composites could efficiently cure western water under almost neutral (pH 6.0) and even slightly alkaline (pH 10.4) conditions [61]. They created an ultrasmall Fe_3O_4 Fenton-like catalyst placed on 3D reduced graphene oxide (rGO). When the weight ratio of GO to Fe_3O_4 is greater than 5%, rGF-5, the upgraded composite enhances the Fenton-like process. The elimination rates of tetracycline hydrochloride (TCH) are 98.7% in 60 minutes and 96.1% in 90 minutes when the initial pH values are 4.5 and 6.7, respectively [62].

Global concern over the presence of antibiotics in drinking water and wastewater is growing; hence, the development of an improved sustainable technique to remove antibiotics from water resources is necessary. Through pyrolysis, MOF-derived Fe^0 embedded in mesoporous carbon was prepared as an efficient heterogeneous Fenton-like catalyst. When tested under different experimental settings, the carbon matrix structure named (FMC) demonstrated enhanced catalytic operation for amoxicillin elimination with a high mineralization efficiency of 60.41%. A thorough evaluation of the catalytic activity of FMC was conducted using a variety of reaction conditions, including temperature, starting pH, and initial H_2O_2 concentration. The function of the reaction in the FMC/ H_2O_2 system was determined, indicating that the assault of hydroxyl radicals ($^{\bullet}OH$) removed amoxicillin [63].

Photo-Fenton process

An improved form of the conventional Fenton process, the photo-Fenton method, involves the inclusion of a second energy source, such as UV radiation. When UV light is added to Fenton's advanced oxidation method for the elimination of organic contaminants, the reaction is recognized as being extremely potent. According to numerous studies, the UV light utilized in the Fenton process enhances the removal of organic contaminants, which is often accomplished by the conventional Fenton process . The addition of UV radiation to the conventional Fenton process causes the photoreduction of ferric ions (Fe^{3+}) to ferrous ions (Fe^{2+}), producing hydroxyl radicals ($^{\bullet}OH$) as opposed to perhydroxyl radicals ($HO_2^{\bullet}$) produced by the traditional Fenton process, as demonstrated in Eq. (1) [64]. Organic pollutant removal efficiency is greatly enhanced by the reaction represented in Eq. (1), which is produced by UV radiation during the photo-Fenton process.

$$Fe^{3+} + H_2O + h\upsilon \rightarrow Fe^{2+} + H^+ + {}^{\bullet}OH \quad (1)$$

Furthermore, like the H_2O_2/UV process, UV irradiation may directly break down H_2O_2 molecules into hydroxyl radicals in the photo-Fenton process. A variety of UV wavelengths (λ = 250–400 nm) can be used for photo-Fenton processes. The rate at which contaminants are destroyed is significantly impacted by the wavelength and intensity of UV radiation. Despite having a comparatively better efficiency than the conventional Fenton process, the photo-Fenton approach has certain intrinsic disadvantages, such as a reduced pH, the production of sediments after treatment, and the inability to recover waste homogeneous catalysts [65].

Some downsides of homogeneous catalysis of photo-Fenton processes include the need to detach iron at the conclusion of the reaction, the creation of sludge, and a limited pH range to prevent iron hydroxide precipitation, which lowers catalyst availability for the reaction. Using iron-based or other heterogeneous catalysts can help mitigate the drawbacks of homogeneous Fenton reactions [66]. To enhance the performance of the photo-Fenton process, heterogeneous nanocatalysts employing heterogeneous photo-Fenton systems with various types of nanomaterials have been developed. With reference to the Fenton advanced oxidation process, new insights have been gained from nanotechnology. Innovative uses of nanomaterials in water treatment have been informed to improve the effectiveness of current treatment procedures and address problems with water quality. This is because of their significant surface area, which results in a high catalytic ability and a large number of reachable reaction sites on the surface, restricting activity loss compared to homogeneous Fenton catalysis [67].

This work involved the synthesis of manganese ferrite. SEM and TEM revealed that $MnFe_2O_4$-R and $MnFe_2O_4$-B were comprised of random-shaped particle agglomerates with different geometries and nanoscale diameters. The heterogeneous photo-Fenton degradation of methylene blue was assessed using manganese ferrites as catalysts. After 120 minutes of treatment, $MnFe_2O_4$-R and $MnFe_2O_4$-B gotten 98% and 92% decolorization, respectively. This study provides a sustainable approach for the production of photocatalytic materials for wastewater treatment [68]. Sodium dodecyl sulfate (SDS), an anionic surfactant, was removed via a photo-Fenton-like oxidation reaction using a unique heterojunction $ZnO/FeVO_4$ nanocatalyst that was made using a straightforward technique. Utilizing 40 mg of the nanocomposite and 1.57 mL of H_2O_2 at pH

5.5 for 45 minutes, the maximum SDS removal efficiency (99.0%) was attained. The produced nanocomposite demonstrated greater catalytic activity in the breakdown of SDS than did the pure $FeVO_4$ and ZnO nanocatalysts. Additionally, the catalyst was effectively used to remediate actual wastewater that contained surfactants. Future applications in environmental remediation seem promising for the ZnO/ $FeVO_4$ nanocatalyst attributable to its high catalytic activity, ease of production, and remarkable reusability. The development of nanocomposites has received increasing attention because of their special qualities. This heterogeneous photo-Fenton-like system for the degradation of methylene blue (MB) was created in barium M-hexaferrites with the novel composition $BaFe_{11}(SnMg)_{0.25}Nd_{0.5}O_{19}$ (SMN). In a pH range of up to 140 minutes, the photo-Fenton-like activity of the SMN-NPs showed strong degradation (98.89%) and mineralization (83%) in the SMN-NPs + H_2O_2 + UV irradiation system. Furthermore, the SMN-NPs showed high stability and recycling potential, and the catalyst was successfully applied to clean real wastewaters [69]. The sol-gel method has been utilized to generate cerium ferrite perovskites (Mg/Ce ferrite perovskites) that substitute magnesium for methylene blue. The results showed that Mg/Ce ferrite perovskites may be developed as superior photo-Fenton catalysts with a 99% capacity to degrade dyes [70]. A hollow-nanotube carbon nitride (Cu-HNCN) catalyst was created and employed in the photo-Fenton (PF) process to degrade organic pollutants. CuNx sites were distributed throughout the hollow nanotube-like structure. The Cu-HNCN/PF system effectively degraded several antibiotic pollutants and broke down tetracycline with 96.0% efficiency in 50 minutes. Furthermore, in the Cu-HNCN/PF system, the short Cu-N bonds increased stability and reduced copper leaching. With the goal of improving the use of the PF process in wastewater purification, this work offers fresh perspectives on the creation of catalysts with high stability and rapid electron transfer. To improve catalytic performance, catalysts with several active sites should be fully used. Due to their high charge mobility and greater number of active sites, 0D/2D hybrids, particularly quantum dots (QDs)/nanosheets (NSs), have drawn significant interest for use in enhanced oxidation processes [71]. g-C_3N_4 nanosheets connected to Cu-Fe bimetallic oxide QDs were created using an easy one-step synthesis method. The optical characteristics and charge separation were efficiently promoted by the interaction of the Cu-Fe sites. In the Fenton method, the coordination of Cu-Fe sites on CNNSs results in a trade-off between H_2O_2 adsorption and activation, which results in exceptional tetracycline removal efficiency throughout a broad pH range [72].

Photocatalysis

Photocatalysis theory is based on the redox capacity of photocatalysts when exposed to light. In contrast to other treatment approaches that use light irradiation and a light-absorbing photocatalyst to accomplish simultaneous oxidation and reduction, heterogeneous photocatalysis is used. Many substances can undergo catalytic photolysis under light irradiation to cause redox reactions [73]. When a photocatalytic material is subjected to light with an energy greater than or equal to the bandgap of the photocatalyst, during the photocatalytic AOP phase, photon absorption results in the formation of pairs of highly reactive electron vacancy electrons (e^-) in the conduction band and holes (h^+) in the valence band. While h^+ participates in the oxidation process in the VB, the photoexcited electrons in the CB encourage reduction processes [74]. This may cause the activation of dissolved oxygen and hydrogen gas, which would create active radicals (such as hydroxyl radicals). In water-based media, h^+ and $^{\cdot}OH$ further breakdown different contaminants to produce CO_2 and H_2O. Figure 17 shows the mechanism of photocatalysis and pollutant degradation [75].

Photocatalysts consisting of semiconductor materials are employed to accelerate redox processes in photocatalytic processes because of their electronic structure. Semiconductors act as catalysts to break down organic pollutants into CO_2 and H_2O [76]. Even though there are several heterogenous photocatalyst materials (such as Fe_2O_3, WO_3, ZrO_2, SnO_2, CdS, ZnS, etc.) with photocatalytic qualities, among the catalysts employed in AOPs, titanium dioxide (TiO_2) is highly efficient. TiO_2 is the most popular semiconductor photocatalyst material; it is nontoxic, recyclable, and ecologically friendly, is less expensive than other materials, and has high chemical stability [77].

Titanium dioxide has been shown to be a very powerful degrading agent when applied to immobilized support. The catalyst effectively removed three azo dyes, C.I. acid orange 10, 12, and 8, also known as AO10, AO12, and AO8, respectively. The color was completely removed, and AO10 showed the best reaction kinetics and energy requirements. The three commercial dyes were practically completely removed from the dyes in less

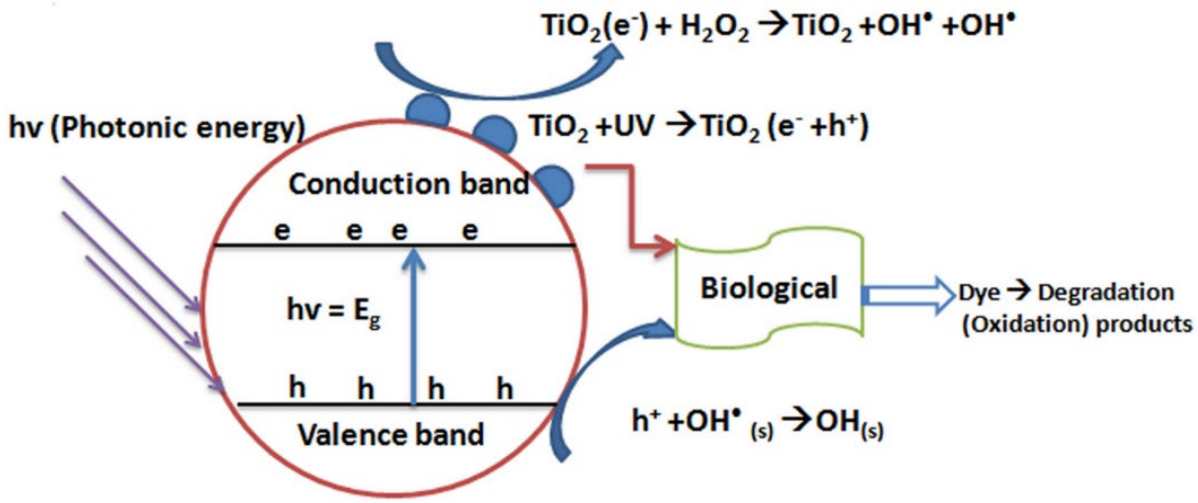

Figure 17. General mechanism degradation of organic dye compounds using the photocatalytic and biological approach [*75*].

than six hours, demonstrating the efficiency of TiO_2. TiO_2 nanoparticles have also been used to successfully break down the color of methylene blue; 100% degradation was accomplished in a matter of hours. The performance dramatically improved when TiO_2 was present at the micro- and nanoscales. An increase in the mass of the TiO_2 catalyst used was attended by an increase in the photocatalyst's effectiveness [78].

By combining photocatalyst materials with the right co catalyst as in Table 1, their capacity to absorb visible light could be improved. The most researched doped photocatalyst is N-doped TiO_2, which can be stimulated by visible light because of its bandgap energy of approximately 2.5 eV [79]. When exposed to visible light, this visible light–active photocatalyst has been shown to be effective in removing several organic compounds from water and wastewater. Research has demonstrated that N-doped TiO_2 exhibits superior photocatalytic performance compared to that of pure titanium dioxide. The use of N-doped TiO_2 results in time-dependent methylene blue degradation and spiroamycin degradation, indicating enhanced photocatalytic activity [80]. Additionally, the impact of N-doped TiO_2 photocatalysis on the inactivation of an *Escherichia coli* strain resistant to antibiotics that was chosen from an effluent from biologically treated urban wastewater was studied. When an antibiotic-resistant *E. coli* strain was placed in biologically treated wastewater, the N-doped TiO_2 photocatalyst showed greater photocatalytic inactivation efficiency than the commercial photocatalyst [66].

By employing a solvothermal calcination procedure to combine Bi_2MoO_6 with TiO_2, antibiotics can be efficiently extracted from aqueous solution. In this case, the TiO_2 conduction band assists as a basis for electron transport, helping charge separation at the contact. This approach can eliminate ciprofloxacin, tetracycline, and oxytetracycline at rates of 88%, 78%, and 78%, respectively, within 150 minutes [81].

Persulfate activation

Most organic molecules in water and wastewater can rapidly and non-selectively oxidized and degraded by $SO_4^{\bullet-}$, which are vigorous oxidizing radicals with redox potentials (E°) of 2.5–3.1 V depending on the activation technique. AOPs based on $SO_4^{\bullet-}$ have attracted a lot of attention because of their distinctive features. The most commonly used activation techniques include ultrasound irradiation , carbon materials , thermal treatment , UV treatment , microwave treatment , and photochemical treatment [95]. One well-known and efficient activation technique for persulfate activation is the usage of TMs. Many TMs, including Cu^{2+}, Mn^{2+}, Ce^{3+}, Ni^{2+}, V^{3+}, Ru^{3+}, and Co^{2+}, have proven successful in activating the persulfate oxidation process because they may function as electron donors to persulfate for the generation of $SO_4^{\bullet-}$ [96]. An appropriate oxidant must first be activated to produce sulfate radicals. Thus, peroxymonosulfate (PMS) and persulfate (PS) are two of the most potent oxidants used in environmental applications. Metallic-based catalysts for PS or PMS activation have garnered increasing interest since they are affordable, require less energy, and can be easily scaled up in practical applications.

Table 1. Different photocatalysts against diverse organic pollutants.

Catalyst	Band gap	Dopant	Pollutant	Efficiency	References
TiO_2	3.0–3.2 eV	Sn & F	Methylene orange dye	77%	[200]
			Methylene blue dye	85%	[201]
			Organic dyes		[202]
		R beads	CIP	92.97%	[203]
Fe_2O_3	2.2 eV	$Ag/ZnFe_2O_4/Ag/BiTa1\text{-}xVxO_4$	Sulphanilamide antibiotic	100%	[204]
		Mg-Zn	Methylene blue dye		[205]
		Sn, CeO_2	Sudan I dye	55%	[206]
WO3	2.4–2.8 eV	ZnS	Pharmaceuticals and personal care products	20–70%	[207]
		Ag	Tetracycline hydrochloride		[208]
Bi_2O_3	2.8 eV	WO_3	e-Norfloxacin	94.58%	[209]
		WO_3	Norfloxacin	88.40%	[210]
ZnO	3.37 eV	$Ag/Fe_2O_3/ZnO$	Ciprofloxacin	76.40%	[211]
			Rhodamine B dye	75%	[212]

It may be used in both homogeneous and heterogeneous systems (Eqs. (2) and (3)) [97].

$$S_2O_8^{2-} + M^n \rightarrow M^{n+1} + SO_4^{\bullet-} + SO_4^{2-} \quad (2)$$

$$HSO_5^{-} + M^n \rightarrow M^{n+1} + SO_4^{\bullet-} + OH^{-} \quad (3)$$

While homogeneous metal-based catalysis provides a quick reaction process, there are several limitations for homogenous systems. First, there is a chance that secondary pollution from leached metals could make it harder to retrieve the catalyst from the treated water. Second, high concentrations of metal ions are needed for wastewater with high levels of organic contaminants, which results in a high concentration of metal ions in the effluent. Third, the pH and water composition have a significant impact on the species of TMs [98]. Metal ions have the potential to precipitate under basic conditions and transform into hydrated species under acidic conditions, hence reducing their activation of metal ions. Furthermore, the presence of organic matter or other chemicals can mix with metal ions to influence PS and PMS activation. A heterogeneous system for PS/PMS activation was created to address the problems. This allows the solid catalyst to be more simply separated from treated wastewater for recycle and has a higher tolerance for harsh operating conditions [99].

In the case of heterogeneous metal activators including zero-valent iron, one of the most useful materials for the remediation of water and wastewater is zero-valent iron (ZVI) which possesses a redox potential of (Fe^0, E^0 = −0.44 V), functions as a potent reductant for oxidants such as PMS and PDS. It has been proven that ZVI uses both homogeneous and heterogeneous persulfate activation pathways to provide ferrous ions. Through direct electron transfer from its surface to PMS/PDS, ZVI can heterogeneously activate persulfate anions, and the ferrous ions released from ZVI can homogeneously degrade PMS/PDS (Eqs. (4) and (5)) [100].

$$Fe + 2S_2O_8^{2-} \rightarrow Fe^{2+} + 2SO_4^{\bullet-} + 2SO_4^{2-} \quad (4)$$

$$Fe + HSO_5^{-} \rightarrow Fe^{2+} + 2SO_4^{\bullet-} + 2OH^{-} \quad (5)$$

Because Fe ions are nontoxic, inexpensive, and ecologically benign, they have also been the subject of extensive research, as have their oxides. Eqs. (6) and (7) demonstrate that Fe^{2+}-activated PS and PMS are among the most effective mechanisms for the production of sulfate radicals [101].

$$Fe^{2+} + S_2O_8^{2-} \rightarrow Fe^{3+} + 2SO_4^{-} + 2SO_4^{2-} \quad (6)$$

$$Fe^{2+} + HSO_5^{-} \rightarrow Fe^{3+} + OH^{-} + SO_4^{\bullet-} \quad (7)$$

Cobalt ions are effective in catalyzing PMS (Eq. (8)). It was discovered that using of cobalt ions (Co^{2+}) as a catalyst for PMS activation might lead to the breakdown of paracetamol. It has been also reported that tetrabromobisphenol A may be broken down by the Co(II)/PMS system's production of sulfate radicals [102].

$$Co^{2+} + HSO_5^{-} \rightarrow Co^{3+} + OH^{-} + SO_4^{\bullet-} \quad (8)$$

The primary concern with the use of cobalt for PMS activation is that large doses of cobalt may be biologically harmful and carcinogenic, despite cobalt being introduced as a nonhazardous substance. As a result, research has been conducted on the heterogeneous form of cobalt, while restrictions have been placed on the homogeneous form. Cobalt-ferrite ($CoFe_2O_4$) is the most advantageous heterogeneous form of cobalt, outperforming Co_3O_4. Because of the strong Fe-Co interactions, the divalent cobalt in $CoFe_2O_4$ can outweigh cobalt leaching. demonstrated that using Co_3O_4/GO for PMS activation greatly decreased cobalt leaching compared to Co_3O_4 [103].

Physical AOPs Process

Electrohydraulic discharge (Plasma)

The fourth state of matter, known as plasma, is an entirely or partially ionized gas. Deeply held electrodes provide powerful electric fields that cause electrical discharge in water, which creates plasma. Based on the plasma-phase distribution, the process of decontaminating wastewater through high-voltage electrical discharge can be broadly classified into three types: electrical discharge above the liquid surface, interfacial plasma-liquid discharge, and direct electrical liquid discharge (Figure 18) [104]. Plasma is formed in each case by the interaction of electricity with the surrounding liquid or air, which results in the synthesis of active substances, including oxidizing radicals ($^{\cdot}OH$, $SO_4^{\cdot-}$, $^1O_2$, and $O_2^{\cdot-}$), active species, UV radiation, and shockwaves, and molecules (O_3, H_2O_2) produced by electric discharge all donate to the breakdown of chemical pollutants [105].

Ultrasound

Ultrasonic frequencies are oscillations that have a frequency greater than 20 kHz and are not often sensed by humans. Ultrasonic reactions typically occur between 20 and 100 kHz to breakdown chemical pollutants, sonochemistry uses sonic cavitation to create free radicals. Two essential phases are involved in the entire process: the creation of radicals within the cavitation bubble and their subsequent dispersion into the bulk solution [106]. When using ultrasound, the expansion and implosive collapse of bubbles or cavities in wastewater are induced by a series of compression and rarefaction cycles caused by ultrasonic waves, which outcomes the formation of $^{\bullet}OH$ radicals. This process occurs at extremely high temperatures (>5000 K) and pressures (>1000 bar). When bubbles or holes collapse, energy is released, which speeds up the decomposition of organic contaminants (Figure 19) [107]. Combining Fenton and ultrasonic irradiation (sono-Fenton process), ultrasound with UV irradiation (sonophotolysis), ultrasonication with catalysts (TiO_2) (sonocatalysis), and photocatalysis and ultrasonic irradiation (sonophotocatalysis) can significantly increase the rate of decomposition of organic pollutants. These mechanisms work together to boost the production of •OH radicals [108].

Microwave

The Microwave (MW) is a portion of electromagnetic spectrum that appears between 300 MHz and 300 GHz in frequency and a wavelength of 1–0.001 m. Microwaves are one of the best ways to help breakdown impurities in wastewater and produce drinkable water. Microwave technology primarily employs the thermal and nonthermal effects of microwaves in the treatment of sewage. Microwave catalyst absorption, which can result in a lot of hot spots that can increase the speed at which compounds react, is primarily responsible for the thermal effect of microwaves. The coupling effect of microwaves and a catalyst with a great wave absorption capacity is primarily responsible for the nonthermal effect [109]. This catalyst can generate hydroxyl radicals with high oxidation potentials, which can accelerate the oxidation of organic molecules. As a result, microwave technology can dramatically shorten reaction times and activation energies. microwaves have been employed in conjunction with oxidants (H_2O_2) or granular activated carbon (GAC)/CuO_x catalysts to help destroy organic contaminants. AOPs based on hydroxyl radicals (HR-AOPs) are proven techniques with excellent efficiency. The most common source of $^{\bullet}OH$ is H_2O_2, Among the most effective and pure oxidants used in water treatment. MW irradiation can break down H_2O_2 to create $^{\bullet}OH$. The MW-H_2O_2 system is an effective tool for eliminating contaminants from the environment. By inducing molecular electronic vibrations, microwave radiation accelerates the temperature rise of the system and increases the generation of free radicals [110]. Within certain bounds, increasing the MW power makes it easier to produce $^{\bullet}OH$ and remove contaminants.

Advantages and limitations of conventional AOPs

Over the last three decades, researchers have extensively investigated the effectiveness of AOPs in treating various challenging wastewaters with persistent and harmful pollutants [111]. AOPs, including various combinations, are known for generating powerful hydroxyl radicals (OH). These processes significantly enhance the breakdown efficiency of impurities in textile wastewater while also lowering overall treatment costs. Extensive research has demonstrated that AOPs are effective for wastewater treatment. Some key advantages of AOPs include efficient Elimination of Organic Pollutants. AOPs can efficiently break down organic pollutants, leading to their removal from wastewater. Also, they facilitate the conversion of organic compounds into water (H_2O) and carbon dioxide (CO_2). They exhibit low selectivity, making them appropriate for addressing a wide range of pollution

problems. AOPs can serve as effective initial treatment steps, partly or fully breaking down non-biodegradable pollutants before conventional biological treatments. This approach helps reduce overall treatment costs. They are also particularly useful for treating contaminants that are resistant to conventional treatment methods. Among various AOPs, the Fenton-based processes exhibit the lowest median electrical energy per order (EEO) value of 0.98 kWh/m³ order⁻¹. This makes the Fenton process cost-effective due to minimal energy input and low reagent costs. Table 2 summarizes the advantages of most commonly applied AOPs in water treatment [112].

Cost comparison of different AOPs

The implementation of Advanced Oxidation Processes (AOPs) in industrial settings necessitates a comprehensive evaluation encompassing both technical feasibility and economic viability. Electrical Energy per Order (EEO) serves as a valuable figure of merit for directly assessing and comparing AOPs based on their economic energy consumption. The concept (EEO) has been developed by Bolton and endorsed by the International Union of Pure and Applied Chemistry (IUPAC); it provides a standardized way to assess different AOPs methods. Expressed in units of kilowatt-hours by 1 order of magnitude in 1 cubic meter (kWh m^{-3} $order^{-1}$), EEO signifies the amount of electrical energy needed to reduce a contaminant's concentration in one cubic meter of polluted water by tenfold (one order of magnitude), irrespective of the specific treatment system employed (Eq. (9)) [113].

$$E_{EO} = \frac{P \times t \times 1000}{V \times \log\left(\frac{C_i}{C_f}\right)} \quad (9)$$

Where P is the power (KW) used during AOP, t is the treatment time (h), V is the treated volume (L), Ci and Cf are the initial and final concentrations of the pollutant (mg L^{-1}). The values of E_{EO} depend heavily on pollutant properties like pH and oxidant concentration [114]. Consequently, E_{EO} values for a specific AOP can exhibit significant variation across multiple orders of magnitude. Even accounting for the inherent variability introduced by diverse laboratory conditions, substantial differences in E_{EO} values remain observable. Figure 20 shows a comparative study investigating (E_{EO}) values of various advanced oxidation processes (AOPs) for textile wastewater treatment. The analysis, based on 241 data points, identified Fenton-based AOPs as the most efficient method in terms of energy consumption (0.98 kWh m^{-3} $order^{-1}$), followed by photochemical (3.20 kWh m^{-3} $order^{-1}$), ozonation (3.34 kWh m^{-3} $order^{-1}$), electrochemical AOP (EAOP) (29.5 kWh m^{-3} $order^{-1}$), photocatalysis (91 kWh m^{-3} $order^{-1}$), and US (971.45 kWh m^{-3} $order^{-1}$), respectively. These findings are consistent with previous research by Miklos et al, who reported a similar order of E_{EO} values for AOPs, with US exhibiting the highest energy demand [115].

Hence the Fenton process is more cost effective to run for treating textile wastewater because the chemicals are affordable, and it doesn't use much energy. This makes it a good choice for big treatment plants. Conversely, heterogeneous photocatalysis processes, despite extensive research efforts, are currently less cost-effective than homogeneous photochemical or ozonation treatments for textile wastewater. This disparity may be attributed to limitations in mass transfer of pollutants to the catalyst surface and a lower quantum yield in photocatalytic reactions responsible for hydroxyl radical (˙OH) generation. Consequently, heterogeneous photocatalysis has limited real-world application in industrial textile wastewater treatment plants [115]. An important distinction exists between removal efficiency and energy consumption within wastewater treatment processes. Azbar et al. exemplify this concept by comparing the cost-effectiveness of various advanced oxidation processes (AOPs) for treating dye effluents from polyester and acetate fibers. While all investigated AOPs (including O_3, UV/H_2O_2, UV/O_3, UV/H_2O_2/O_3, and Fenton) achieved significant color removal (90%), required operating costs of 5.28, 1.26, 6.38, 6.54, and 0.23 \$ m^{-3}, respectively. Although the UV/H_2O_2/O_3 process demonstrated the highest level of pollutant removal (chemical oxygen demand, COD), the Fenton process emerged as the most cost-effective option [116].

Limitation of catalyst

AOPs have emerged as a potentially transformative technology for the treatment of recalcitrant pollutants present in textile industry wastewater and landfill leachate. However, their widespread implementation is currently impeded by several technical and economic considerations. Research has identified shortcomings in using hydroxyl radical-based AOPs as a pre-treatment step for biological treatment of landfill leachate. These limitations hinder the effectiveness of AOPs in this application [117].

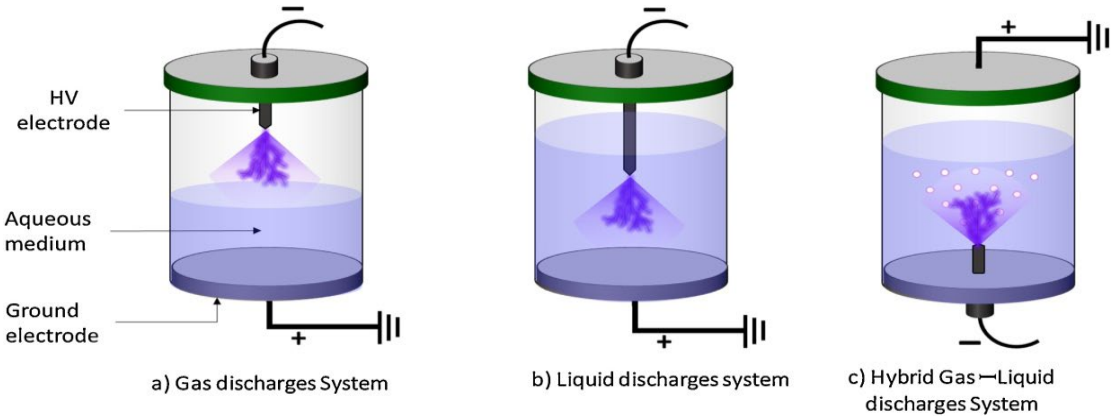

Figure 18. Diagram showing the many discharge plasma systems used to treat water [104].

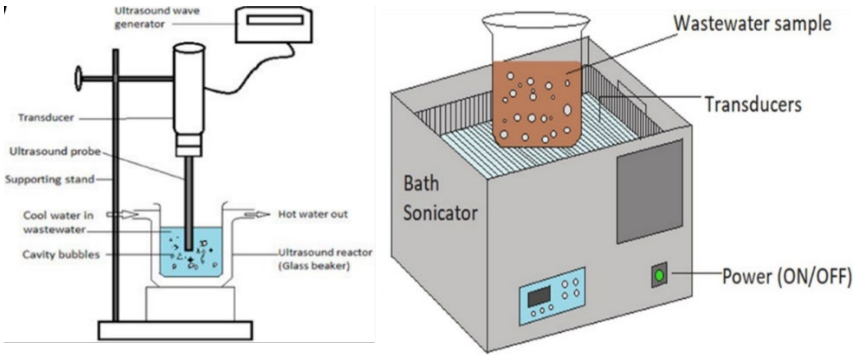

Figure 19. Types of Sonicators (a) probe sonicator, and (b) Bath tub sonicator [107].

Table 2. Advantages of applied AOPs in wastewater treatment.

AOPs	Advantages
H_2O_2/UV	Disinfectant; simple process.
Electrochemical-based processes	Eco-friendly, Powerful hydroxyl radical and automatable.
Fenton-based process	Fast, compact, and affordable: Offers rapid degradation, small footprint, and cost-effective operation. It is also powerful and versatile via generating strong oxidants to break down a wide range of pollutants. Simple and sustainable: Avoids mass transfer steps.
O_3/H_2O_2/UV	It works on all chemicals in the solution and breaks down aromatics and polyphenols much faster.
O_3/H_2O_2	More efficient than O_3 or H_2O_2 alone; effective for H_2O treatment.
O_3/UV	More efficient treatment, especially for ·OH generation. Outperforms standalone ozone or UV.
O_3	Powerful, Fast & Clean: Ozone offers strong oxidation, requires minimal setup, works quickly, leaves no sludge, and decomposes naturally.

A primary goal of applying AOPs is to improve the biodegradability of leachate, making it more amenable to breakdown by microorganisms in subsequent biological treatment stages. However, studies have shown that AOPs often fall short in this regard. The BOD5/COD ratio, a key indicator of biodegradability, remains low (below 0.50 in most cases) following AOP treatment. This suggests that AOPs may not be an optimal pre-treatment choice for biological processes. Another major challenge is the ineffectiveness of hydroxyl radicals in removing ammonia nitrogen, another prevalent pollutant in landfill leachate. Hydroxyl radicals react very slowly with ammonia, hindering the ability of AOPs to address this crucial contaminant [118]. Given these constraints, it's important to explore alternative pre-treatment methods. Furthermore, AOPs may generate toxic byproducts or leave behind residual oxidants (e.g., hydrogen peroxide) that can negatively affect microbial activity. Therefore, optimizing the dosage of chemical oxidants employed in the AOP stage is critical.

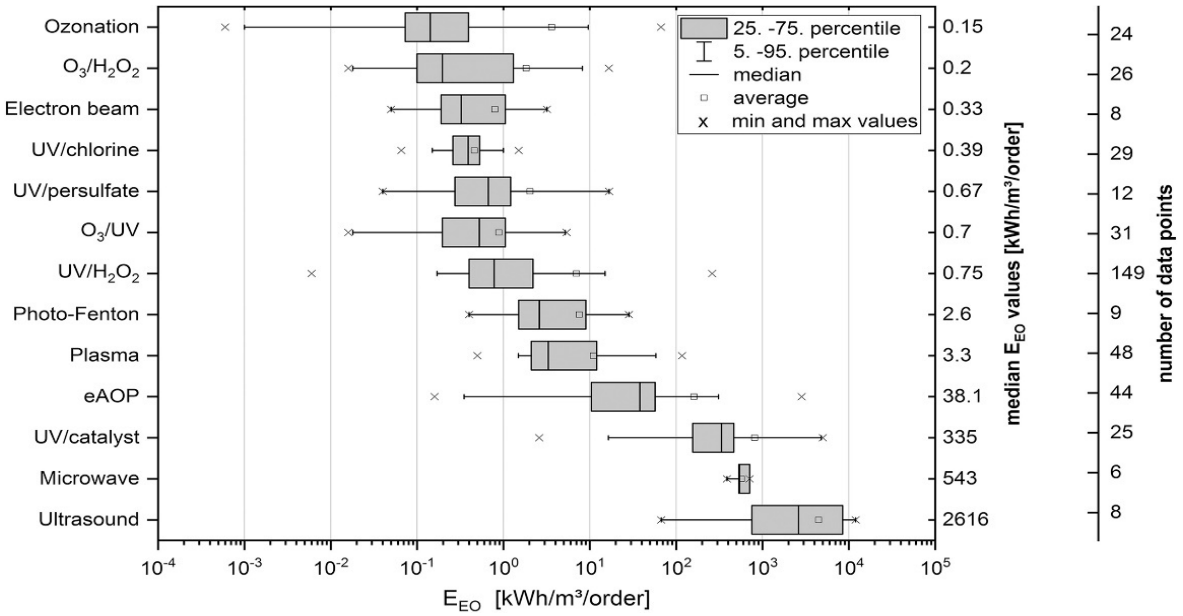

Figure 20. EEO values of various AOPs on textile wastewater treatment [*115*].

This optimization aims to achieve a balance between effective pollutant degradation and minimizing detrimental effects on subsequent biological treatment [119].

Formation of by-products

In some cases, AOPs can generate harmful byproducts during the degradation process. These byproducts may include partially oxidized organic compounds or inorganic transformation products. For example, certain AOPs can lead to the formation of nitrates or bromates, which themselves require further treatment or removal due to potential health or environmental concerns. It is crucial that treatment reduces the overall harmfulness or toxicity of the effluent. This is because the treatment process itself might create new byproducts that are even more hazardous than the original pollutants. For instance, some treatments can generate long-lasting intermediate compounds that are more toxic than the dyes they were derived from [112].

Industrial-scale applications

While advanced oxidation processes (AOPs) demonstrate remarkable success at the laboratory scale, their translation to full-scale industrial applications necessitates further research. Economic feasibility and operational efficiency remain critical factors limiting widespread AOP adoption within the industrial sector [112]. The successful transition of AOPs from laboratory-scale experiments to industrial applications necessitates addressing critical engineering complexities. These complexities include ensuring uniform reactant distribution, achieving efficient mixing, and optimizing reactor design to address hydrodynamics, mass transfer, and heat transfer phenomena. Among the challenges stood against the industrial-scale application of the process are the dynamic Hydroxyl Radical Production consequently the effectively adapting AOPs to accommodate the fluctuating wastewater volumes encountered in industrial settings remains a hurdle, the high cost of reagents and energy consumption associated with AOPs and the real-Time Efficiency Monitoring due to The lack of rapid and in-situ methods for measuring Hydroxyl radical production efficiency within AOP systems. However the development of portable and low-cost continuous-flow reactors offers a potentially transformative solution for overcoming these scalability challenges [120].

Incomplete Mineralization

While AOPs excel at breaking down complex molecules, they might not always achieve complete mineralization, the process where pollutants are entirely converted to harmless end products like carbon dioxide and water. This can leave behind residual organic matter that may require further biological treatment or disposal. The extent of mineralization achieved depends on the specific AOP employed, operating conditions, and the characteristics of the pollutants present.

CONCLUSIONS

This review synthesizes current knowledge on using recycled transition metals from batteries for tannery wastewater purification. The incorporation of various transition metals into advanced oxidation processes (AOPs) has demonstrated their potential for sustainable water treatment, particularly due to their enhanced performance against recalcitrant dyes. While promising results have been reported across various treatment techniques, the use of transition metals in aqueous solutions still presents challenges, including the formation of byproducts. This suggests may open doors for researchers to use composites such as polymers or some reticular structures like MOFs to guarantee fewer metal atoms get released into the solution.

REFERENCES

[1] S. Naghdi, M.M. Shahrestani, M. Zendehbad, H. Djahaniani, H. Kazemian, D. Eder, Recent advances in application of metal-organic frameworks (MOFs) as adsorbent and catalyst in removal of persistent organic pollutants (POPs), Journal of Hazardous Materials, 442 (2023) 130127.

[2] W. Gong, L. Bai, H. Liang, Membrane-based technologies for removing emerging contaminants in urban water systems: Limitations, successes, and future improvements, Desalination, 590 (2024) 117974.

[3] S. Dey Chowdhury, R.Y. Surampalli, P. Bhunia, Advanced Oxidation Processes for Microconstituents Removal in Aquatic Environments, Microconstituents in the Environment: Occurrence, Fate, Removal and Management, (2023) 367-404.

[4] X. Sun, P. Wei, Z. He, F. Cheng, L. Tang, Q. Li, J. Han, J.J.J.o.A. He, Compounds, Novel transition-metal phosphides@ N, P-codoped carbon electrocatalysts synthesized via a universal strategy for overall water splitting, 932 (2023) 167253.

[5] E.C. Okpara, O.C. Olatunde, O.B. Wojuola, D.C. Onwudiwe, Applications of transition metal oxides and chalcogenides and their composites in water treatment: a review, Environmental Advances, 11 (2023) 100341.

[6] R.A. Fideles, A.B. Mageste, L.L.B.S. Nascimento, G.M.D. Ferreira, H.P. Neves, L.R. de Lemos, G.D. Rodrigues, G.M.D.J.T.T.i.A.C. Ferreira, Aqueous two-phase systems for the extraction, separation, and recovery of synthetic dyes, (2024) 117652.

[7] N. Hemashenpagam, S. Selvajeyanthi, Textile dyes and their effect on human beings, Nanohybrid materials for treatment of textiles dyes, Springer2023, pp. 41-60.

[8] T. Yu, H. Chen, T. Hu, J. Feng, W. Xing, L. Tang, W.J.A.C.B.E. Tang, Recent advances in the applications of encapsulated transition-metal nanoparticles in advanced oxidation processes for degradation of organic pollutants: A critical review, 342 (2024) 123401.

[9] Y. Zhang, N. Zhang, J. Chen, T. Zhang, W. Ge, W. Zhang, G. Xie, L. Zhang, Y.J.J.o.A. He, Compounds, Preparation and lithium storage properties of C@ TiO2/3D carbon hollow sphere skeleton composites, 815 (2020) 152511.

[10] W.T. Yein, Q. Wang, D.-S.J.C. Kim, Piezoelectric catalytic driven advanced oxidation process using two-dimensional metal dichalcogenides for wastewater pollutants remediation, (2024) 141524.

[11] F. Cao, X. Yang, C. Shen, X. Li, J. Wang, G. Qin, S. Li, X. Pang, G.J.J.o.m.c.A. Li, Electrospinning synthesis of transition metal alloy nanoparticles encapsulated in nitrogen-doped carbon layers as an advanced bifunctional oxygen electrode, 8 (2020) 7245-7252.

[12] C. Wang, R. Deng, M. Guo, Q.J.I.j.o.h.e. Zhang, Recent progress of advanced Co3O4-based materials for electrocatalytic oxygen evolution reaction in acid: from rational screening to efficient design, (2023).

[13] H. Wang, J. Li, K. Li, Y. Lin, J. Chen, L. Gao, V. Nicolosi, X. Xiao, J.-M.J.C.S.R. Lee, Transition metal nitrides for electrochemical energy applications, 50 (2021) 1354-1390.

[14] F.-Z. Zhang, X.-B. Liu, C.-M. Yang, G.-D. Chen, Y. Meng, H.-B. Zhou, S.-H.J.M.T. Zhang, Insights into robust carbon nanotubes in tribology: From nano to macro, (2024).

[15] M. Zubair, M.M.U. Hassan, M.T. Mehran, M.M. Baig, S. Hussain, F.J.I.J.o.H.E. Shahzad, 2D MXenes and their heterostructures for HER, OER and overall water splitting: a review, 47 (2022) 2794-2818.

[16] G. Moon, N. Lee, S. Kang, J. Park, Y.-E. Kim, S.-A. Lee, R.K. Chitumalla, J. Jang, Y. Choe, Y.-K. Oh, Hydrothermal synthesis of novel two-dimensional α-quartz nanoplates and their applications in energy-saving, high-efficiency, microalgal biorefineries, Chemical Engineering Journal, 413 (2021) 127467.

[17] H. Niu, Y. Zheng, S. Wang, L. Zhao, S. Yang, Y. Cai, Continuous generation of hydroxyl radicals for highly efficient elimination of chlorophenols and phenols catalyzed by heterogeneous Fenton-like catalysts yolk/shell Pd@ Fe3O4@ metal organic frameworks, Journal of hazardous materials, 346 (2018) 174-183.

[18] Q. Xia, Z. Jiang, D. Li, J. Wang, Z. Yao, Green synthesis of a dendritic Fe3O4@ Feo composite modified with polar C-groups for Fenton-like oxidation of phenol, Journal of Alloys and Compounds, 746 (2018) 453-461.

[19] K. Anwar, F.K. Naqvi, S. Beg, Facile hydrothermal synthesis of Yb doped Bi4V2O11 nanoparticles for the improvement of photocatalytic and AC impedance performance: Investigation of polymorphism, adsorption isotherm, optical properties and possible mechanism with the help of GCMS, Journal of Alloys and Compounds, 938 (2023) 168483.

[20] V.A. Naik, V.A. Thakur, Hydrothermal synthesis of Fe3O4@ rGO@ CdS/Bi2S3 nanocomposite as an

efficient, recyclable magnetic photocatalyst for photo-Fenton dye degradation and chromium VI reduction under sunlight, Inorganic Chemistry Communications, 160 (2024) 111962.
[21] S.-J. Huang, A. Muneeb, P. Sabhapathy, A. Sheelam, K.S. Bayikadi, R. Sankar, Tailoring the Co 4+/Co 3+ active sites in a single perovskite as a bifunctional catalyst for the oxygen electrode reactions, Dalton Transactions, 50 (2021) 7212-7222.
[22] Y. Shen, Catalytic pyrolysis of biomass with char modified by cathode materials of spent lithium-ion batteries for tar reduction and syngas production, Fuel, 316 (2022) 123321.
[23] Z. Cao, C. Zuo, Direct synthesis of magnetic CoFe2O4 nanoparticles as recyclable photo-fenton catalysts for removing organic dyes, ACS omega, 5 (2020) 22614-22620.
[24] Q. Shen, Q. Song, C. Xiao, Q. Fu, W. Li, S. Zhang, H. Li, Ultrahigh thermal conductive graphite film via the in-situ construction of aligned nanographene skeleton using chemical vapor deposition, Journal of Materials Science & Technology, 148 (2023) 1-9.
[25] C. Dai, B. Li, J. Li, B. Zhao, R. Wu, H. Ma, X. Duan, Controllable synthesis of NiS and NiS 2 nanoplates by chemical vapor deposition, Nano Research, 13 (2020) 2506-2511.
[26] V. Pavlenko, S. Żółtowska, A. Haruna, M. Zahid, Z. Mansurov, Z. Supiyeva, A. Galal, K. Ozoemena, Q. Abbas, T. Jesionowski, A comprehensive review of template-assisted porous carbons: Modern preparation methods and advanced applications, Materials Science and Engineering: R: Reports, 149 (2022) 100682.
[27] Q. Cai, F. Wang, Y. Hou, Y. Jia, B. Liao, B. Shen, D. Zhang, Core-shell materials for selective catalytic reducing of NOx with ammonia: Synthesis, anti-poisoning performance, and remaining challenges, Fuel Processing Technology, 243 (2023) 107675.
[28] E. Doustkhah, R. Hassandoost, A. Khataee, R. Luque, M.H.N. Assadi, Hard-templated metal–organic frameworks for advanced applications, Chemical Society Reviews, 50 (2021) 2927-2953.
[29] M.-H. Kim, D.-H. Park, J.-H. Byeon, D.-M. Lim, Y.-H. Gu, S.-H. Park, K.-W. Park, Fe-doped Co3O4 nanostructures prepared via hard-template method and used for the oxygen evolution reaction in alkaline media, Journal of Industrial and Engineering Chemistry, 123 (2023) 436-446.
[30] Y. Wu, C. Ye, L. Yu, Y. Liu, J. Huang, J. Bi, L. Xue, J. Sun, J. Yang, W. Zhang, Soft template-directed interlayer confinement synthesis of a Fe-Co dual single-atom catalyst for Zn-air batteries, Energy Storage Materials, 45 (2022) 805-813.
[31] X. Chen, D. Kang, J. Li, T. Zhou, H.J.J.o.h.m. Ma, Gradient and facile extraction of valuable metals from spent lithium ion batteries for new cathode materials re-fabrication, 389 (2020) 121887.
[32] X. Chang, M. Fan, C.F. Gu, W.H. He, Q. Meng, L.J. Wan, Y.G.J.A.C.I.E. Guo, Selective extraction of transition metals from spent LiNixCoyMn1− x− yO2 cathode via regulation of coordination environment, 61 (2022) e202202558.
[33] M. Wang, K. Liu, Z. Xu, S. Dutta, M. Valix, D.S. Alessi, L. Huang, J.B. Zimmerman, D.C.J.E.S. Tsang, Technology, Selective extraction of critical metals from spent lithium-ion batteries, 57 (2023) 3940-3950.
[34] X. Jin, P. Zhang, L. Teng, S. Rohani, M. He, F. Meng, Q. Liu, W. Liu, Acid-free extraction of valuable metal elements from spent lithium-ion batteries using waste copperas, Waste Management, 165 (2023) 189-198.
[35] Y. Wang, G. Yu, Challenges and pitfalls in the investigation of the catalytic ozonation mechanism: A critical review, Journal of Hazardous Materials, 436 (2022) 129157.
[36] X. Duan, S. Yang, S. Wacławek, G. Fang, R. Xiao, D.D. Dionysiou, Limitations and prospects of sulfate-radical based advanced oxidation processes, Journal of Environmental Chemical Engineering, 8 (2020) 103849.
[37] F. Tanos, A. Razzouk, G. Lesage, M. Cretin, M. Bechelany, A Comprehensive Review on Modification of Titanium Dioxide-Based Catalysts in Advanced Oxidation Processes for Water Treatment, ChemSusChem, (2023) e202301139.
[38] X. Jin, C. Wu, L. Fu, X. Tian, P. Wang, Y. Zhou, J. Zuo, Development, dilemma and potential strategies for the application of nanocatalysts in wastewater catalytic ozonation: A review, Journal of Environmental Sciences, 124 (2023) 330-349.
[39] J. Ma, M. Sui, T. Zhang, C. Guan, Effect of pH on MnOx/GAC catalyzed ozonation for degradation of nitrobenzene, Water Research, 39 (2005) 779-786.
[40] A.C. Gomes, L.R. Fernandes, R.M. Simões, Oxidation rates of two textile dyes by ozone: Effect of pH and competitive kinetics, Chemical Engineering Journal, 189 (2012) 175-181.
[41] P. Yang, S. Luo, Y. Liu, W. Jiao, Degradation of nitrobenzene wastewater in an acidic environment by Ti (IV)/H 2 O 2/O 3 in a rotating packed bed, Environmental Science and Pollution Research, 25 (2018) 25060-25070.
[42] Z. Guo, Y. Xie, J. Xiao, Z.-J. Zhao, Y. Wang, Z. Xu, Y. Zhang, L. Yin, H. Cao, J.J.J.o.t.A.C.S. Gong, Single-atom Mn–N4 site-catalyzed peroxone reaction for the efficient production of hydroxyl radicals in an acidic solution, 141 (2019) 12005-12010.
[43] S.-P. Tong, W.-w. Li, S.-q. Zhao, C.-a. Ma, Titanium (IV)-improved H2O2/O3 process for acetic acid degradation under acid conditions, Ozone: science & engineering, 33 (2011) 441-448.
[44] L. Chen, H. Li, J. Qian, Degradation of roxarsone in UV-based advanced oxidation processes: A comparative study, Journal of Hazardous Materials, 410 (2021) 124558.

[45] T. Meng, X. Su, P. Sun, W. Sun, D. Santoro, H. Yao, H. Wang, UV-based advanced oxidation processes in photoreactors with reflective sleeves, Journal of Cleaner Production, 416 (2023) 137945.
[46] E. Bein, B. Seiwert, T. Reemtsma, J.E. Drewes, U. Hübner, Advanced oxidation processes for removal of monocyclic aromatic hydrocarbon from water: Effects of O3/H2O2 and UV/H2O2 treatment on product formation and biological post-treatment, Journal of Hazardous Materials, 450 (2023) 131066.
[47] A. Seidmohammadi, R. Amiri, J. Faradmal, M. Lili, G. Asgari, UVA-LED assisted persulfate/nZVI and hydrogen peroxide/nZVI for degrading 4-chlorophenol in aqueous solutions, Korean Journal of Chemical Engineering, 35 (2018) 694-701.
[48] L. Škodič, S. Vajnhandl, J. Volmajer Valh, T. Željko, B. Vončina, A. Lobnik, Comparative study of reactive dyes oxidation by H2O2/UV, H2O2/UV/Fe2+ and H2O2/UV/Fe Processes, Ozone: Science & Engineering, 39 (2017) 14-23.
[49] V. Dubois, C.S. Rodrigues, A.S. Alves, L.M. Madeira, UV/vis-based persulphate activation for p-nitrophenol degradation, Catalysts, 11 (2021) 480.
[50] S. Dhaka, R. Kumar, M.A. Khan, K.-J. Paeng, M.B. Kurade, S.-J. Kim, B.-H. Jeon, Aqueous phase degradation of methyl paraben using UV-activated persulfate method, Chemical Engineering Journal, 321 (2017) 11-19.
[51] K. Krawczyk, S. Wacławek, E. Kudlek, D. Silvestri, T. Kukulski, K. Grübel, V.V. Padil, M. Černík, UV-catalyzed persulfate oxidation of an anthraquinone based dye, Catalysts, 10 (2020) 456.
[52] N.T. Hoang, V.T. Nguyen, N.D.M. Tuan, T.D. Manh, P.-C. Le, D. Van Tac, F.M. Mwazighe, Degradation of dyes by UV/Persulfate and comparison with other UV-based advanced oxidation processes: Kinetics and role of radicals, Chemosphere, 298 (2022) 134197.
[53] L. Feng, E.D. van Hullebusch, M.A. Rodrigo, G. Esposito, M.A. Oturan, Removal of residual anti-inflammatory and analgesic pharmaceuticals from aqueous systems by electrochemical advanced oxidation processes. A review, Chemical Engineering Journal, 228 (2013) 944-964.
[54] A.V. Karim, P.V. Nidheesh, M.A. Oturan, Boron-doped diamond electrodes for the mineralization of organic pollutants in the real wastewater, Current Opinion in Electrochemistry, 30 (2021) 100855.
[55] S. Yu, R. Zhang, Y. Dang, Y. Zhou, J.-J.J.S. Zhu, P. Technology, Electrochemical activation of peroxymonosulfate at Ti/La2O3-PbO2 anode to enhance the degradation of typical antibiotic wastewater, 294 (2022) 121164.
[56] C. Yan, L.J.J.o.h.m. Liu, Oxidation of gas phase ammonia via accelerated generation of radical species and synergy of photo electrochemical catalysis with persulfate activation by CuO-Co3O4 on cathode electrode, 388 (2020) 121793.
[57] J.-P. Zou, Y. Chen, S.-S. Liu, Q.-J. Xing, W.-H. Dong, X.-B. Luo, W.-L. Dai, X. Xiao, J.-M. Luo, J.J.W.r. Crittenden, Electrochemical oxidation and advanced oxidation processes using a 3D hexagonal Co3O4 array anode for 4-nitrophenol decomposition coupled with simultaneous CO2 conversion to liquid fuels via a flower-like CuO cathode, 150 (2019) 330-339.
[58] N. Wang, T. Zheng, G. Zhang, P. Wang, A review on Fenton-like processes for organic wastewater treatment, Journal of Environmental Chemical Engineering, 4 (2016) 762-787.
[59] T. Yu, H. Chen, T. Hu, J. Feng, W. Xing, L. Tang, W. Tang, Recent advances in the applications of encapsulated transition-metal nanoparticles in advanced oxidation processes for degradation of organic pollutants: A critical review, Applied Catalysis B: Environmental, 342 (2024) 123401.
[60] R. Yang, Q. Peng, B. Yu, Y. Shen, H. Cong, Yolk-shell Fe3O4@ MOF-5 nanocomposites as a heterogeneous Fenton-like catalyst for organic dye removal, Separation and Purification Technology, 267 (2021) 118620.
[61] L. Lyu, M. Han, W. Cao, Y. Gao, Q. Zeng, G. Yu, X. Huang, C. Hu, Efficient Fenton-like process for organic pollutant degradation on Cu-doped mesoporous polyimide nanocomposites, Environmental Science: Nano, 6 (2019) 798-808.
[62] X. Zhang, Z. Yao, Y. Zhou, Z. Zhang, G. Lu, Z. Jiang, Theoretical guidance for the construction of electron-rich reaction microcenters on C–O–Fe bridges for enhanced Fenton-like degradation of tetracycline hydrochloride, Chemical Engineering Journal, 411 (2021) 128535.
[63] W. Xie, Z. Huang, F. Zhou, Y. Li, X. Bi, Q. Bian, S. Sun, Heterogeneous fenton-like degradation of amoxicillin using MOF-derived Fe0 embedded in mesoporous carbon as an effective catalyst, Journal of Cleaner Production, 313 (2021) 127754.
[64] K.H.H. Aziz, F.S. Mustafa, K.M. Omer, I. Shafiq, Recent advances in water falling film reactor designs for the removal of organic pollutants by advanced oxidation processes: a review, Water Resources and Industry, (2023) 100227.
[65] X. Wang, X. Zhang, Y. Zhang, Y. Wang, S.-P. Sun, W.D. Wu, Z. Wu, Nanostructured semiconductor supported iron catalysts for heterogeneous photo-Fenton oxidation: a review, Journal of materials chemistry A, 8 (2020) 15513-15546.
[66] V. Vaiano, D. Sannino, O. Sacco, The use of nanocatalysts (and nanoparticles) for water and wastewater treatment by means of advanced oxidation processes, Nanotechnology in the Beverage Industry, Elsevier2020, pp. 241-264.
[67] D. Sannino, V. Vaiano, P. Ciambelli, L.A. Isupova, Structured catalysts for photo-Fenton oxidation of acetic acid, Catalysis Today, 161 (2011) 255-259.
[68] V. Morais, R. Barrada, M. Moura, J. Almeida, T. Moreira, G. Gonçalves, S. Ferreira, M. Lelis, M. Freitas,

Synthesis of manganese ferrite from spent Zn–MnO2 batteries and its application as a catalyst in heterogeneous photo-Fenton processes, Journal of Environmental Chemical Engineering, 8 (2020) 103716.

[69] G.A. Ashraf, M. Hassan, R.T. Rasool, W. Abbas, L. Zhang, Mesoporous SnMgNd substituted M-hexaferrite catalyzed heterogeneous photo-Fenton-like activity for degradation of methylene blue, Journal of colloid and interface science, 557 (2019) 408-422.

[70] A. Anantharaman, B.A. Josephine, V.M. Teresita, T. Ajeesha, M. George, Photo-Fenton activity of magnesium substituted cerium ferrite perovskites for degradation of methylene blue via sol–gel method, Journal of nanoscience and nanotechnology, 19 (2019) 5116-5129.

[71] L. Su, P. Wang, X. Ma, J. Wang, S. Zhan, Regulating local electron density of iron single sites by introducing nitrogen vacancies for efficient photo-fenton process, Angewandte Chemie, 133 (2021) 21431-21436.

[72] M. Liu, H. Xia, W. Yang, X. Liu, J. Xiang, X. Wang, L. Hu, F. Lu, Novel Cu-Fe bi-metal oxide quantum dots coupled g-C3N4 nanosheets with H2O2 adsorption-activation trade-off for efficient photo-Fenton catalysis, Applied Catalysis B: Environmental, 301 (2022) 120765.

[73] J.J. Rueda-Marquez, I. Levchuk, P.F. Ibañez, M. Sillanpää, A critical review on application of photocatalysis for toxicity reduction of real wastewaters, Journal of Cleaner Production, 258 (2020) 120694.

[74] L. Xiong, J. Tang, Strategies and challenges on selectivity of photocatalytic oxidation of organic substances, Advanced Energy Materials, 11 (2021) 2003216.

[75] T.G. Ambaye, K. Hagos, Photocatalytic and biological oxidation treatment of real textile wastewater, Nanotechnology for Environmental Engineering, 5 (2020) 1-11.

[76] A.G. Akerdi, S.H. Bahrami, Application of heterogeneous nano-semiconductors for photocatalytic advanced oxidation of organic compounds: A review, Journal of Environmental Chemical Engineering, 7 (2019) 103283.

[77] Z. Li, S. Wang, J. Wu, W. Zhou, Recent progress in defective TiO2 photocatalysts for energy and environmental applications, Renewable and Sustainable Energy Reviews, 156 (2022) 111980.

[78] K. Bisaria, S. Sinha, R. Singh, H.M. Iqbal, Recent advances in structural modifications of photo-catalysts for organic pollutants degradation–a comprehensive review, Chemosphere, 284 (2021) 131263.

[79] A.K. Chakraborty, S. Ganguli, M.A. Sabur, Nitrogen doped titanium dioxide (N-TiO2): Electronic band structure, visible light harvesting and photocatalytic applications, Journal of Water Process Engineering, 55 (2023) 104183.

[80] O. Sacco, M. Stoller, V. Vaiano, P. Ciambelli, A. Chianese, D. Sannino, Photocatalytic degradation of organic dyes under visible light on N-doped TiO 2 photocatalysts, International Journal of Photoenergy, 2012 (2012).

[81] J. Mukherjee, B.K. Lodh, R. Sharma, N. Mahata, M.P. Shah, S. Mandal, S. Ghanta, B. Bhunia, Advanced oxidation process for the treatment of industrial wastewater: A review on strategies, mechanisms, bottlenecks and prospects, Chemosphere, (2023) 140473.

[82] K. Ancy, C. Vijilvani, M. Bindhu, S.J.S. Bai, K.S. Almaary, T.M. Dawoud, A. Mubarak, M.S. Alfadul, Visible light assisted photocatalytic degradation of commercial dyes and waste water by Sn–F co-doped titanium dioxide nanoparticles with potential antimicrobial application, Chemosphere, 277 (2021) 130247.

[83] N.N. Mohammad Jafri, J. Jaafar, N.H. Alias, S. Samitsu, F. Aziz, W.N. Wan Salleh, M.Z. Mohd Yusop, M.H.D. Othman, M.A. Rahman, A.F. Ismail, Synthesis and characterization of titanium dioxide hollow nanofiber for photocatalytic degradation of methylene blue dye, Membranes, 11 (2021) 581.

[84] Z.M. Shammi, A. Kianfar, M. Momeni, Photocatalytic degradation and mineralization of dye pollutants from wastewater under visible light using synthetic CuO-VO2/TiO2 nanotubes/nanosheets, Journal of Materials Science: Materials in Electronics, 32 (2021) 20149-20163.

[85] L. Pretali, E. Fasani, M. Sturini, Current advances on the photocatalytic degradation of fluoroquinolones: photoreaction mechanism and environmental application, Photochemical & Photobiological Sciences, 21 (2022) 899-912.

[86] R. Wang, J. Tang, X. Zhang, D. Wang, X. Wang, S. Xue, Z. Zhang, D.D. Dionysiou, Construction of novel Z-scheme Ag/ZnFe2O4/Ag/BiTa1-xVxO4 system with enhanced electron transfer capacity for visible light photocatalytic degradation of sulfanilamide, Journal of hazardous materials, 375 (2019) 161-173.

[87] T. Bessy, M. Bindhu, J. Johnson, S.-M. Chen, T.-W. Chen, K.S. Almaary, UV light assisted photocatalytic degradation of textile waste water by Mg0. 8-xZnxFe2O4 synthesized by combustion method and in-vitro antimicrobial activities, Environmental Research, 204 (2022) 111917.

[88] S. Alwera, V.S. Talismanov, V. Alwera, D. Domyati, Synthesis and characterization of Sn-doped CeO2-Fe2O3 nanocomposite and application in photocatalytic degradation of Sudan I, Biointerface Res. Appl. Chem, 13 (2023) 179.

[89] B. Czech, P. Zygmunt, Z.C. Kadirova, K. Yubuta, M. Hojamberdiev, Effective photocatalytic removal of selected pharmaceuticals and personal care products by elsmoreite/tungsten oxide@ ZnS photocatalyst,

Journal of Environmental Management, 270 (2020) 110870.
[90] J. Chen, X. Xiao, Y. Wang, Z. Ye, Ag nanoparticles decorated WO3/g-C3N4 2D/2D heterostructure with enhanced photocatalytic activity for organic pollutants degradation, Applied Surface Science, 467 (2019) 1000-1010.
[91] C. Huang, L. Chen, H. Li, Y. Mu, Z. Yang, Synthesis and application of Bi 2 WO 6 for the photocatalytic degradation of two typical fluoroquinolones under visible light irradiation, RSC advances, 9 (2019) 27768-27779.
[92] T. Jiang, L. Cheng, Y. Han, J. Feng, J. Zhang, One-pot hydrothermal synthesis of Bi2O3-WO3 pn heterojunction film for photoelectrocatalytic degradation of norfloxacin, Separation and Purification Technology, 238 (2020) 116428.
[93] A. Kaur, W.A. Anderson, S. Tanvir, S.K. Kansal, Solar light active silver/iron oxide/zinc oxide heterostructure for photodegradation of ciprofloxacin, transformation products and antibacterial activity, Journal of colloid and interface science, 557 (2019) 236-253.
[94] S. Rajendrachari, P. Taslimi, A.C. Karaoglanli, O. Uzun, E. Alp, G.K. Jayaprakash, Photocatalytic degradation of Rhodamine B (RhB) dye in waste water and enzymatic inhibition study using cauliflower shaped ZnO nanoparticles synthesized by a novel One-pot green synthesis method, Arabian Journal of Chemistry, 14 (2021) 103180.
[95] M.Y. Kilic, W.H. Abdelraheem, X. He, K. Kestioglu, D.D. Dionysiou, Photochemical treatment of tyrosol, a model phenolic compound present in olive mill wastewater, by hydroxyl and sulfate radical-based advanced oxidation processes (AOPs), Journal of hazardous materials, 367 (2019) 734-742.
[96] U. Ushani, X. Lu, J. Wang, Z. Zhang, J. Dai, Y. Tan, S. Wang, W. Li, C. Niu, T. Cai, Sulfate radicals-based advanced oxidation technology in various environmental remediation: a state-of-the–art review, Chemical Engineering Journal, 402 (2020) 126232.
[97] X. Zheng, X. Niu, D. Zhang, M. Lv, X. Ye, J. Ma, Z. Lin, M. Fu, Metal-based catalysts for persulfate and peroxymonosulfate activation in heterogeneous ways: A review, Chemical Engineering Journal, 429 (2022) 132323.
[98] J. Wang, S. Wang, Activation of persulfate (PS) and peroxymonosulfate (PMS) and application for the degradation of emerging contaminants, Chemical Engineering Journal, 334 (2018) 1502-1517.
[99] W.-D. Oh, T.-T. Lim, Design and application of heterogeneous catalysts as peroxydisulfate activator for organics removal: an overview, Chemical Engineering Journal, 358 (2019) 110-133.
[100] A. Hassani, J. Scaria, F. Ghanbari, P. Nidheesh, Sulfate radicals-based advanced oxidation processes for the degradation of pharmaceuticals and personal care products: a review on relevant activation mechanisms, performance, and perspectives, Environmental Research, 217 (2023) 114789.
[101] S. Xiao, M. Cheng, H. Zhong, Z. Liu, Y. Liu, X. Yang, Q. Liang, Iron-mediated activation of persulfate and peroxymonosulfate in both homogeneous and heterogeneous ways: A review, Chemical Engineering Journal, 384 (2020) 123265.
[102] P. Hu, M. Long, Cobalt-catalyzed sulfate radical-based advanced oxidation: a review on heterogeneous catalysts and applications, Applied Catalysis B: Environmental, 181 (2016) 103-117.
[103] D. Zhou, L. Chen, J. Li, F. Wu, Transition metal catalyzed sulfite auto-oxidation systems for oxidative decontamination in waters: A state-of-the-art minireview, Chemical Engineering Journal, 346 (2018) 726-738.
[104] K. Kyere-Yeboah, I.K. Bique, X.-c. Qiao, Advances of non-thermal plasma discharge technology in degrading recalcitrant wastewater pollutants. A comprehensive review, Chemosphere, (2023) 138061.
[105] C.A. Aggelopoulos, Recent advances of cold plasma technology for water and soil remediation: A critical review, Chemical Engineering Journal, 428 (2022) 131657.
[106] K. Peng, F.G. Qin, R. Jiang, W. Qu, Q. Wang, Production and dispersion of free radicals from transient cavitation Bubbles: An integrated numerical scheme and applications, Ultrasonics Sonochemistry, 88 (2022) 106067.
[107] S. Korpe, P.V. Rao, Application of advanced oxidation processes and cavitation techniques for treatment of tannery wastewater—A review, Journal of Environmental Chemical Engineering, 9 (2021) 105234.
[108] S. Mosleh, M. Rahimi, M. Ghaedi, K. Dashtian, Sonophotocatalytic degradation of trypan blue and vesuvine dyes in the presence of blue light active photocatalyst of Ag3PO4/Bi2S3-HKUST-1-MOF: central composite optimization and synergistic effect study, Ultrasonics sonochemistry, 32 (2016) 387-397.
[109] M. Cao, P. Xu, K. Tian, F. Shi, Q. Zheng, D. Ma, G. Zhang, Recent advances in microwave-enhanced advanced oxidation processes (MAOPs) for environmental remediation: A review, Chemical Engineering Journal, (2023) 144208.
[110] H. Xia, C. Li, G. Yang, Z. Shi, C. Jin, W. He, J. Xu, G. Li, A review of microwave-assisted advanced oxidation processes for wastewater treatment, Chemosphere, 287 (2022) 131981.
[111] I. Akmehmet Balcıoğlu, I. Arslan Alaton, M. Ötker, R. Bahar, N. Bakar, M. Ikiz, Application of advanced oxidation processes to different industrial wastewaters, Journal of Environmental Science and Health, Part A, 38 (2003) 1587-1596.
[112] A. Buthiyappan, A.R. Abdul Aziz, W.M.A. Wan Daud, Recent advances and prospects of catalytic advanced

oxidation process in treating textile effluents, Reviews in Chemical Engineering, 32 (2016) 1-47.
[113] J. Casado, Towards industrial implementation of Electro-Fenton and derived technologies for wastewater treatment: A review, Journal of Environmental Chemical Engineering, 7 (2019) 102823.
[114] N. Daneshvar, A. Aleboyeh, A. Khataee, The evaluation of electrical energy per order (EEo) for photooxidative decolorization of four textile dye solutions by the kinetic model, Chemosphere, 59 (2005) 761-767.
[115] D.B. Miklos, C. Remy, M. Jekel, K.G. Linden, J.E. Drewes, U. Hübner, Evaluation of advanced oxidation processes for water and wastewater treatment–A critical review, Water research, 139 (2018) 118-131.
[116] N. Azbar, T. Yonar, K. Kestioglu, Comparison of various advanced oxidation processes and chemical treatment methods for COD and color removal from a polyester and acetate fiber dyeing effluent, Chemosphere, 55 (2004) 35-43.
[117] Y. Deng, Advanced oxidation processes (AOPs) for reduction of organic pollutants in landfill leachate: a review, International Journal of Environment and Waste Management, 4 (2009) 366-384.
[118] S.H. Lin, C.C. Chang, Treatment of landfill leachate by combined electro-Fenton oxidation and sequencing batch reactor method, Water research, 34 (2000) 4243-4249.
[119] K. Paździor, L. Bilińska, S. Ledakowicz, A review of the existing and emerging technologies in the combination of AOPs and biological processes in industrial textile wastewater treatment, Chemical Engineering Journal, 376 (2019) 120597.
[120] H. Noda, K. Oikawa, H. Ohya-Nishiguchi, H. Kamada, Efficient hydroxyl radical production and their reactivity with ethanol in the presence of photoexcited semiconductors, Bulletin of the Chemical Society of Japan, 67 (1994) 2031-2037.